Fermilab

Managed by Fermi Research Alliance, LLC for the U.S. Department of Energy Office of Science

MARS15 Simulations of Particle-Matter Interactions

Nikolai Mokhov

Izabela Szlufarska Visit at Fermilab

November 29, 2018

Outline

- MARS15 Code
- Typical Applications
- Physics Models
- Energy Deposition, Atomic Displacements and Helium Production
- Verification and Code Intercomparison
- Thermal Shock, Ablation and Hydrodynamic Tunneling

MARS15 (mars.fnal.gov)

- MARS15 is a general-purpose **Fortran 77 and C++** code for Monte-Carlo simulations of coupled hadronic and electromagnetic cascades, with heavy ion, muon and neutrino production and interaction. It covers a wide energy range: 1 keV to 100 TeV for muons, hadrons, heavy ions and electromagnetic showers; and 10^{-5} eV to 100 TeV for neutrons.
- Nuclear interactions are described by state-of-the-art LAQGSM, CEM, TENDL and phenomenological models. Nuclide decay, transmutation and resulting activity distribution are calculated with the built-in DeTra code.
- Practically all strong, weak and electromagnetic interactions in the entire energy range can be simulated either inclusively or exclusively, i.e, in a biased mode or in a fully or partially analogue mode.
- ENDF/B-VIII.0(2018) nuclear data are used to handle interactions of neutrons with energies below 14 MeV and derive the NRT/Stoller/Nordlund DPA x-sections below 200 MeV. The elemental distributions are automatically unpacked into isotope distributions for both user-defined and those from the 172 built-in materials.

MARS15: Other Features

- A tagging module allows one to tag the origin of a given signal for source term or sensitivity analyses. Several variance reduction techniques, such as weight windows, particle splitting, and Russian roulette are implemented.
- Six ways to describe geometry are offered, with a basic solid body representation and a ROOT-based powerful engine among them.
- ***The powerful capabilities of MARS15 for simulation in accelerator environment*** with the MARS-MAD Beamline Builder (**MMBLB**) working in concert with an accelerator tracking code (since almost 20 years ago) and with a recent active merge with MADX-PTC for a convenient creation of accelerator models and multi-turn tracking and cascade simulation in accelerator and beamline lattices.
- MARS15 is routinely used in concert with ANSYS for iterative studies of thermo-mechanical problems and can be interfaced to a hydrodynamic code to study phase transition and "**hydrodynamic tunneling**" – first done in 1993 at SSC for a 20-TeV proton beam.

Typical Applications

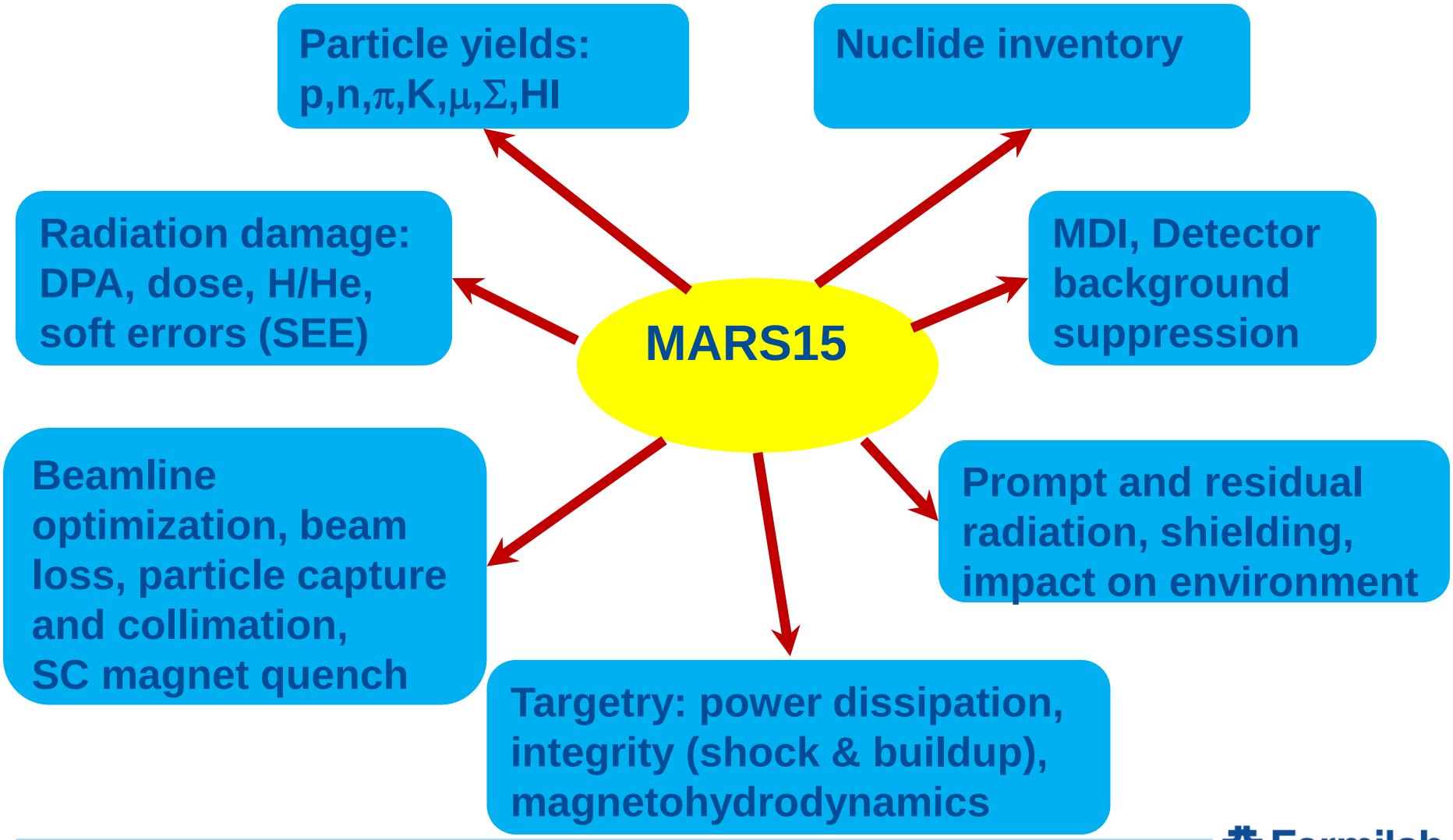

Fermilab

Geometry Description and ROOT-based Beamline Builder

1. User-generated via MARS extended geometry input files
2. User-generated ROOT files
3. GDML files (e.g., a two-way exchange with Geant4 teams)
4. G4beamline's BruitDeFond can generate MARS's input files MARS.INP, GEOM.INP and FIELD.INP
5. STEP files from project CAD models used to generate ROOT geometry modules
6. Lattice and beamline components such as dipole and quadrupole magnets, correctors, accelerating cavities, cryomodules and tunnel with all the details available on geometry, materials and electromagnetic fields by means of the advanced ROOT-based Beamline Builder

Example: MARS-LBNF Model

Target station (TS)

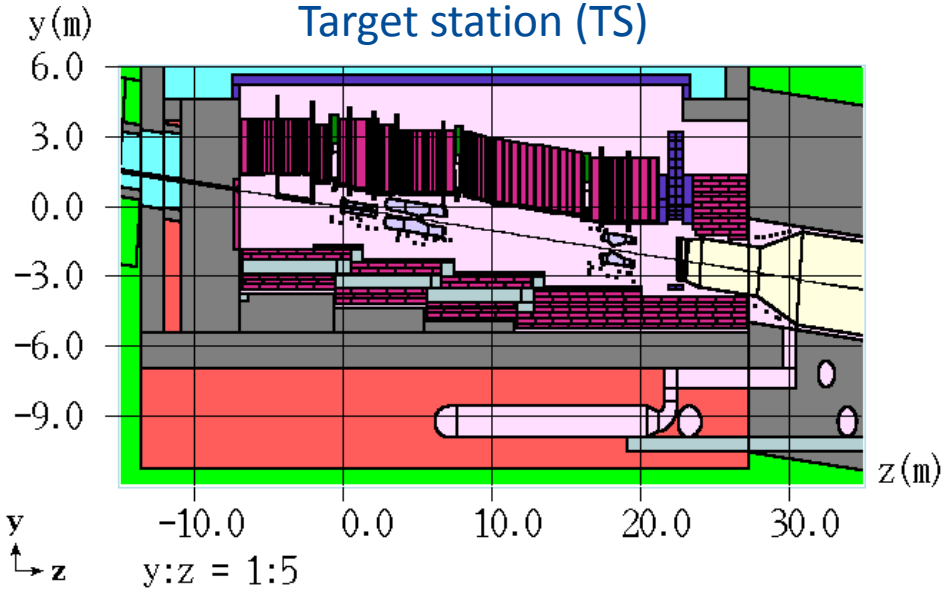

TS, DK and hadron absorber complex

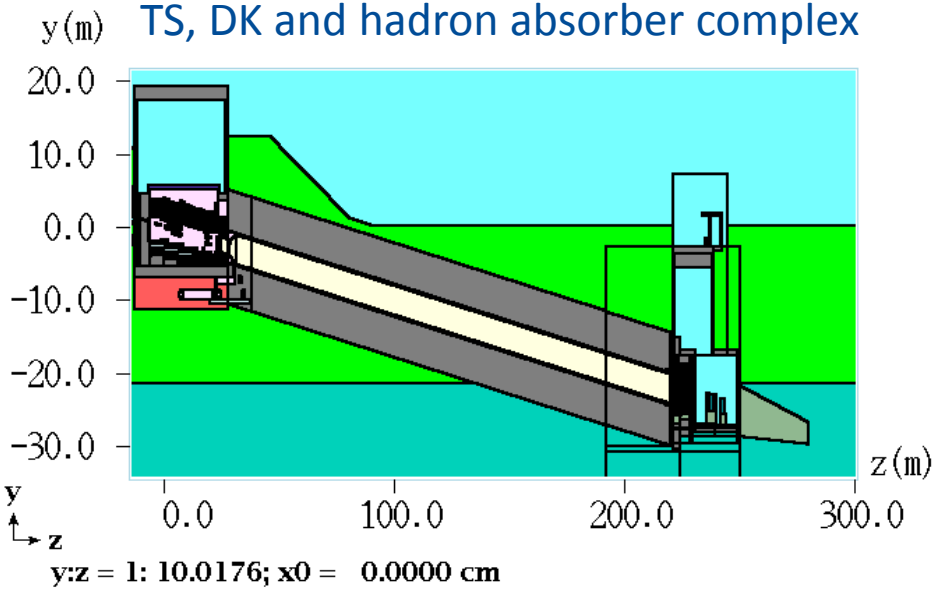

TS Components

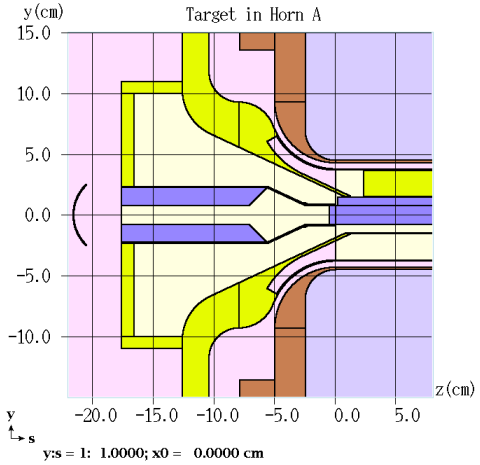

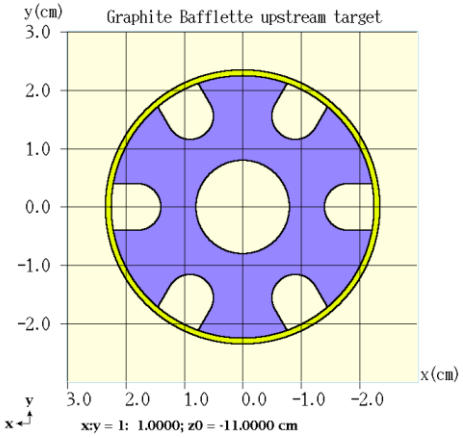

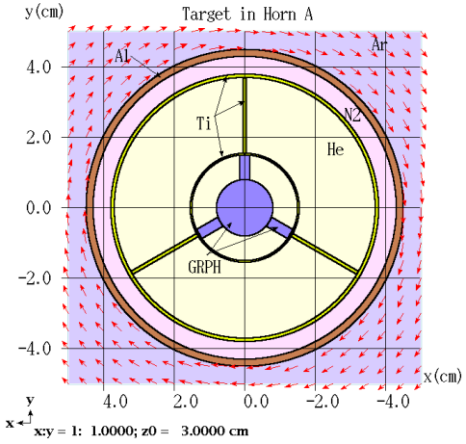

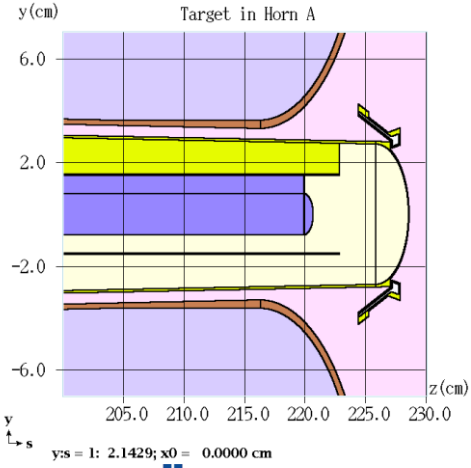

Fermilab

Example: J-PARC 3-GeV Ring MARS Model

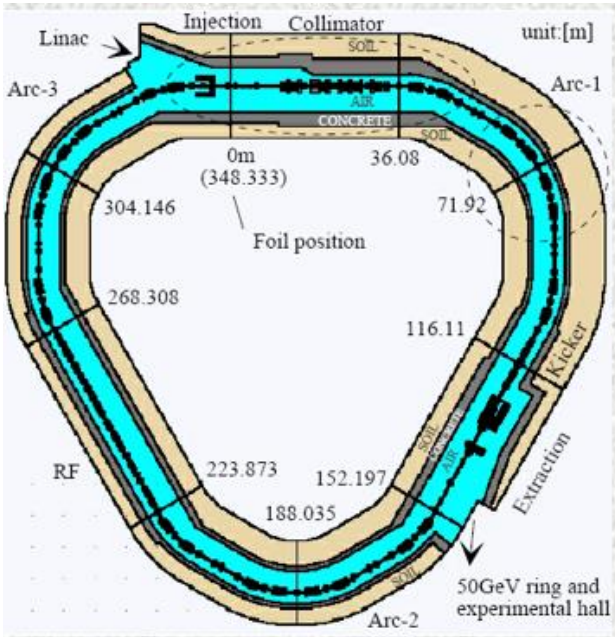

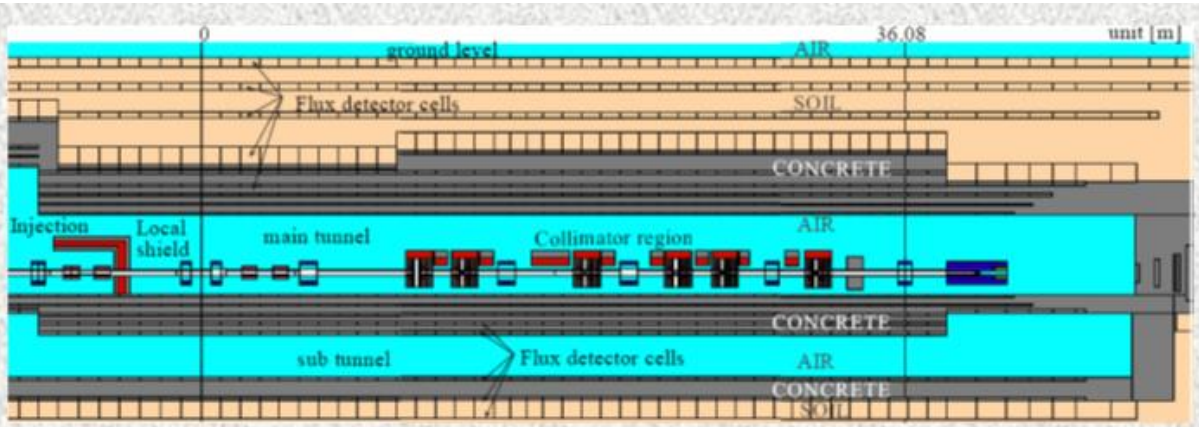

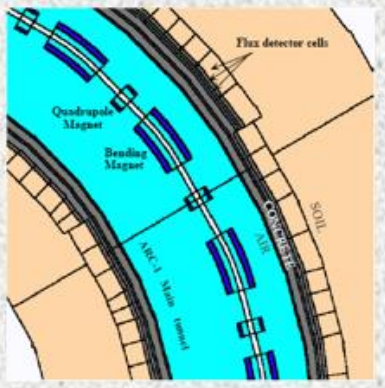

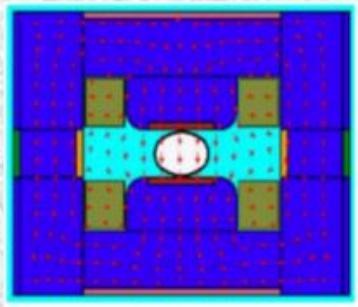

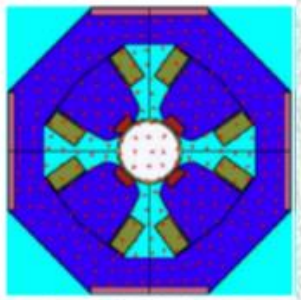

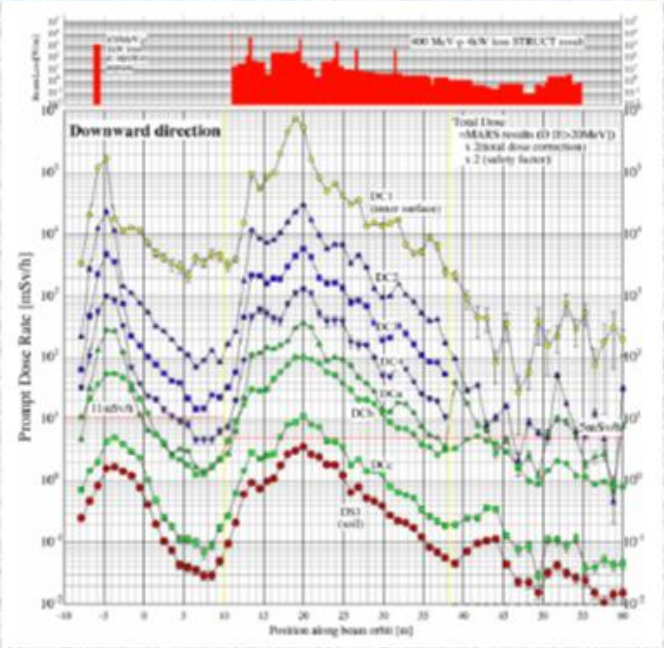

Fermilab

Examples: Fermilab Recycler and ILC

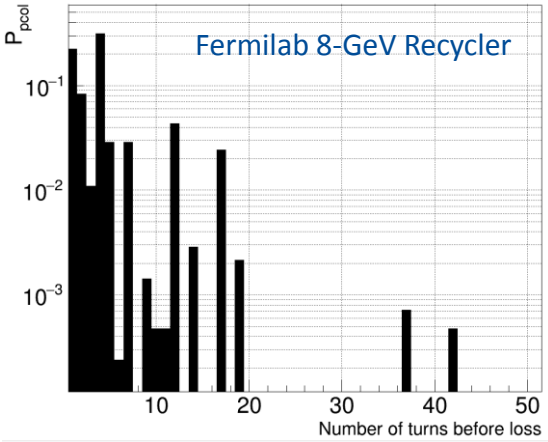

Probability to be lost for beam halo protons passed through the primary collimator vs #turns

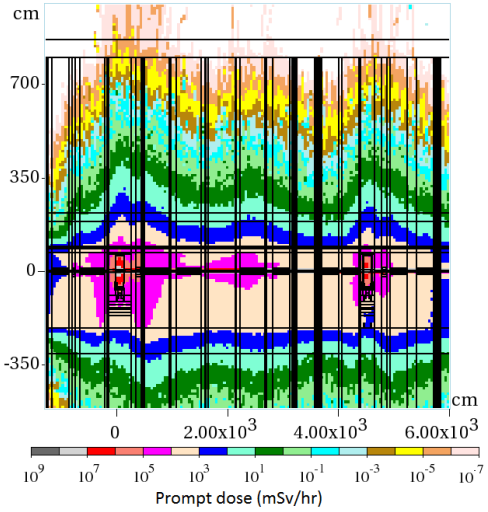

Prompt dose in collimation region

MARS15 SRF model

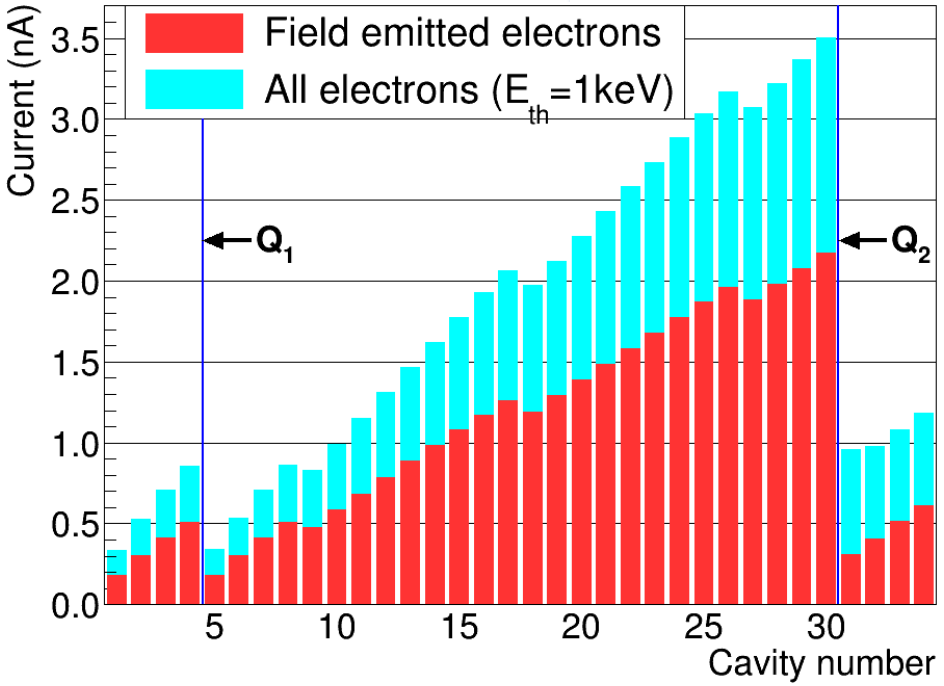

Dark current electrons and EMS electrons in ILC aperture with their loss responsible for radiation load to components and radiation field in ILC tunnel

Fermilab

Nuclear Interaction Cross-Sections

The **first most important quantity** to simulate particle transport by Monte-Carlo method

$$\Sigma(i,A,E) = \frac{\sigma(i,A,E) N_A \, 10^{-27} \, \rho}{A}, \text{ cm}^{-1}$$

where σ is a microscopic x-section (mb) for a given interaction type of a particle of *i*-type with a chosen absorber nucleus with atomic mass A; N_A is Avogadro number (=6.022× 10^{23} mol^{-1}), ρ is density (g/cm^3)

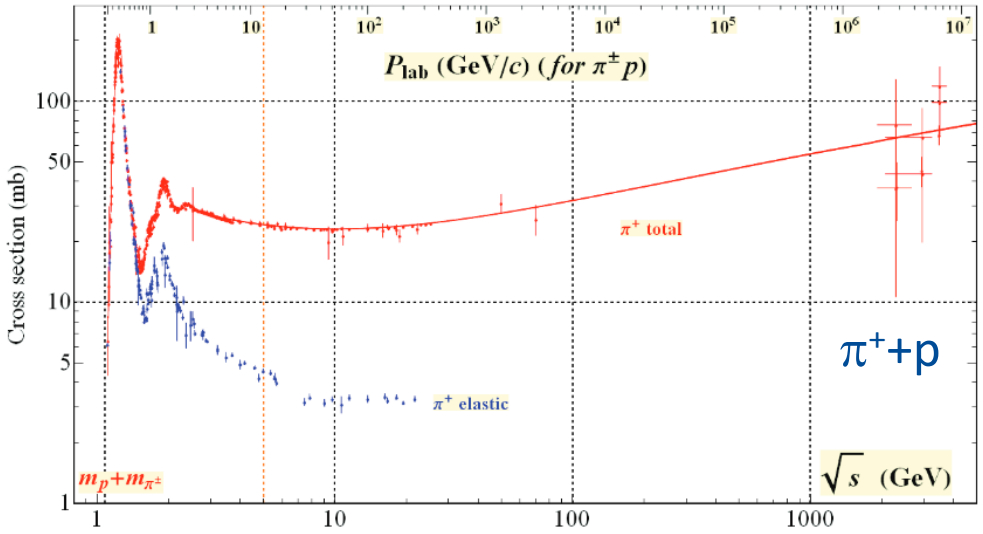

$$s = m_1^2 + m_2^2 + 2E_{1lab}m_2$$

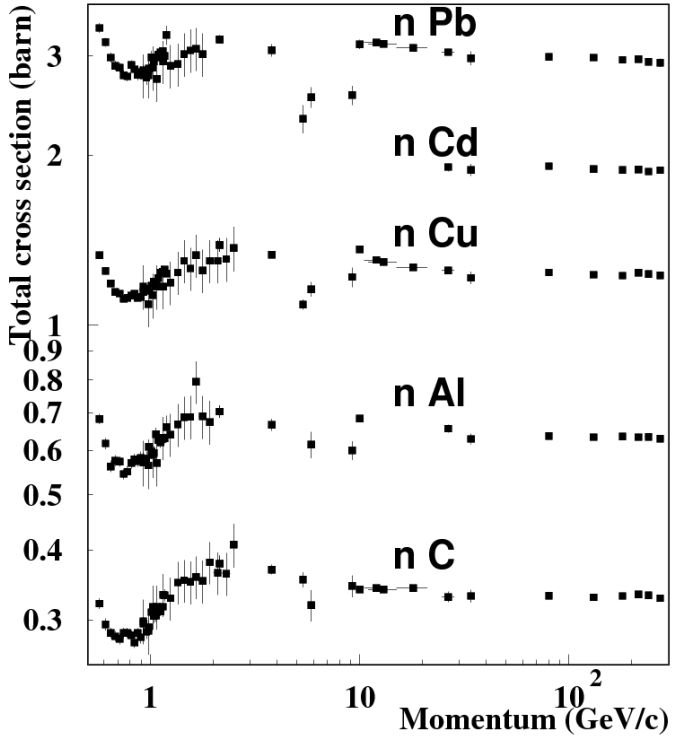

Fermilab

Low-Energy Neutron-Nucleus Cross-Sections

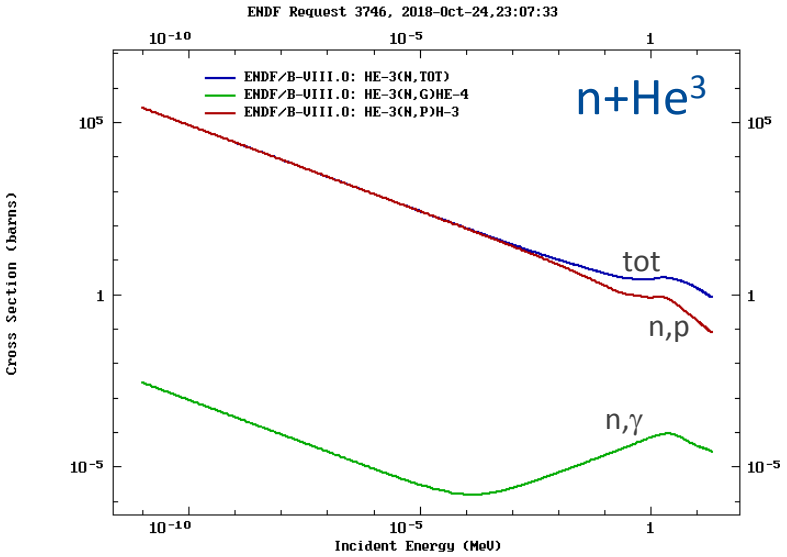

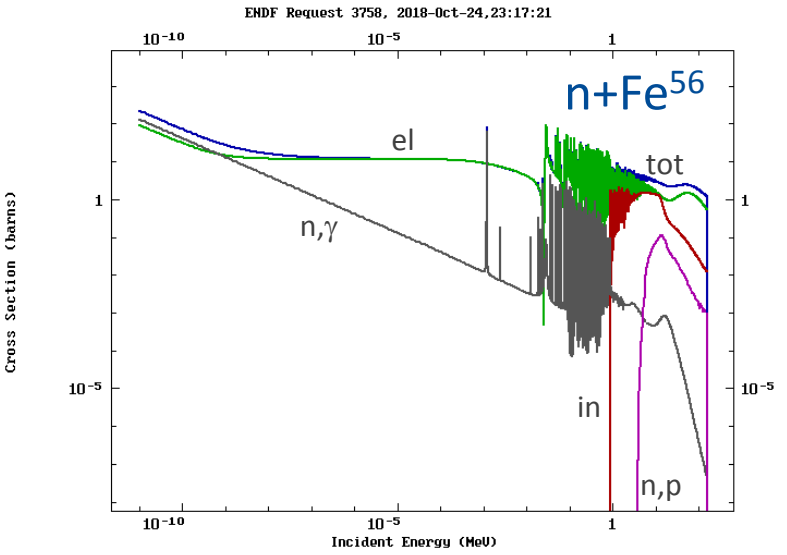

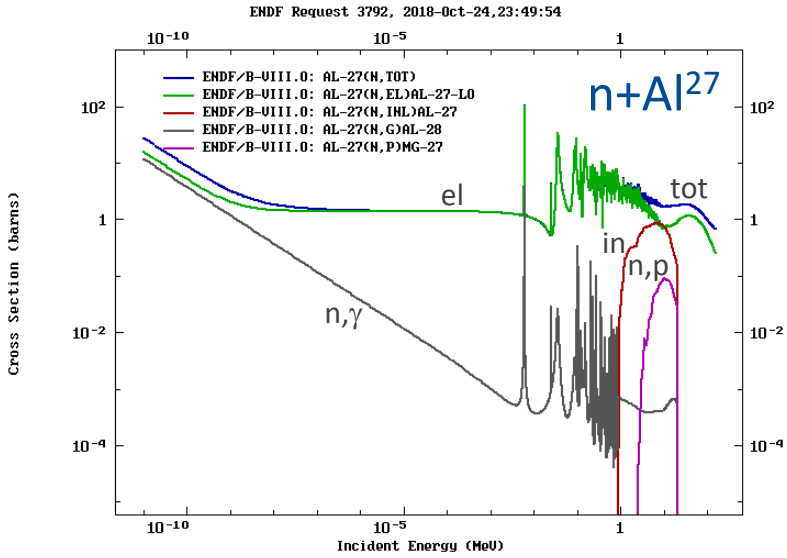

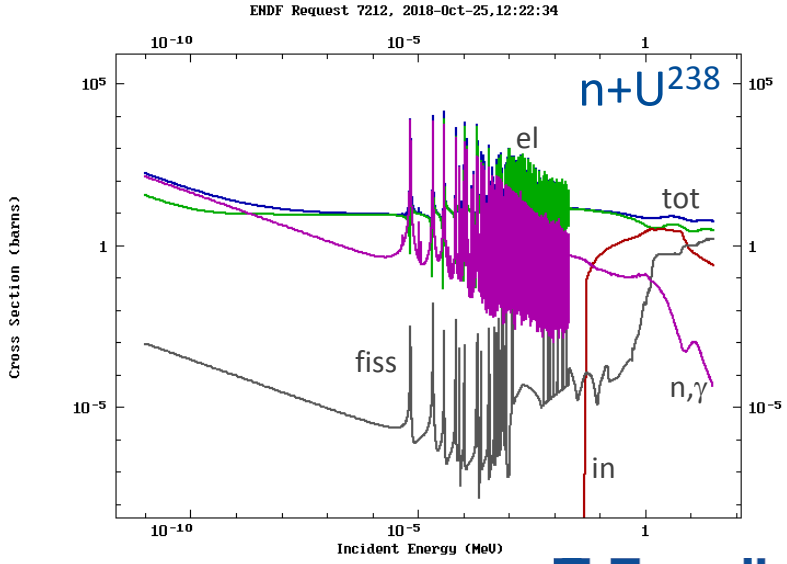

Fermilab

LAQGSM vs HARP-CDP at 8GeV/c and KaoS at 3.5GeV

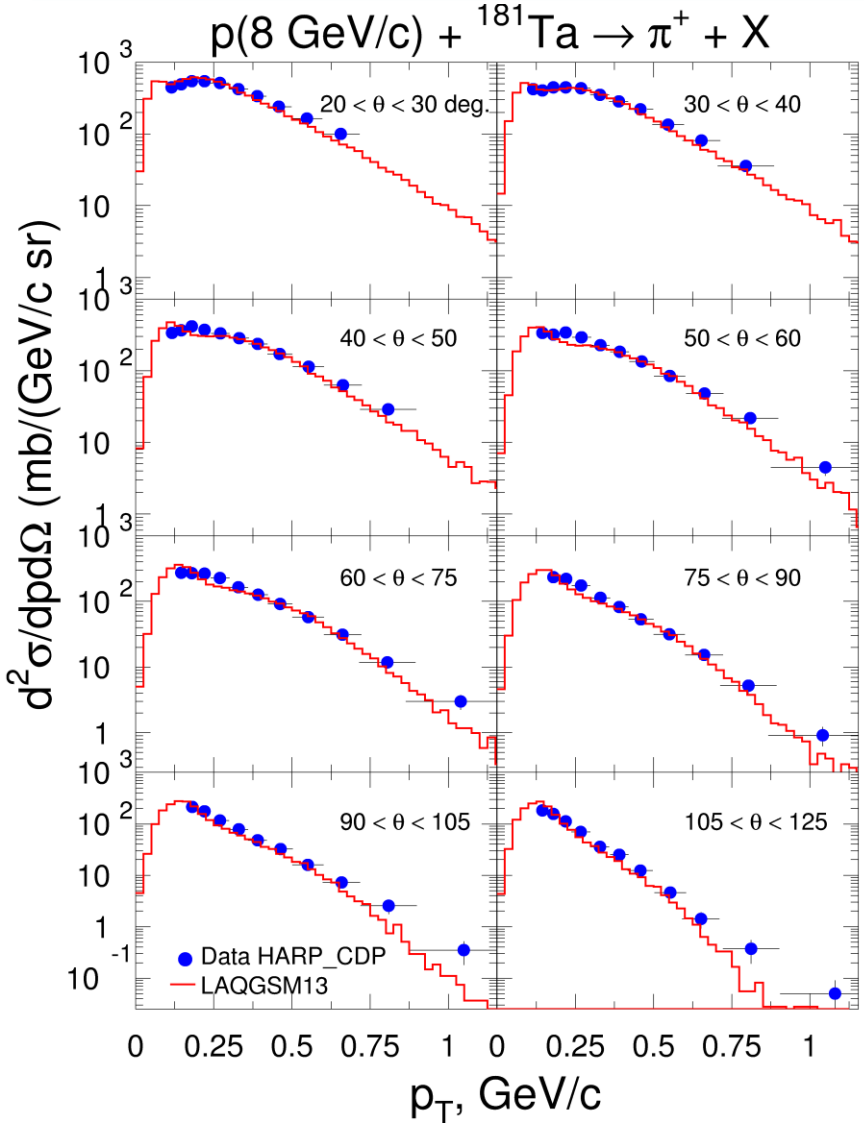

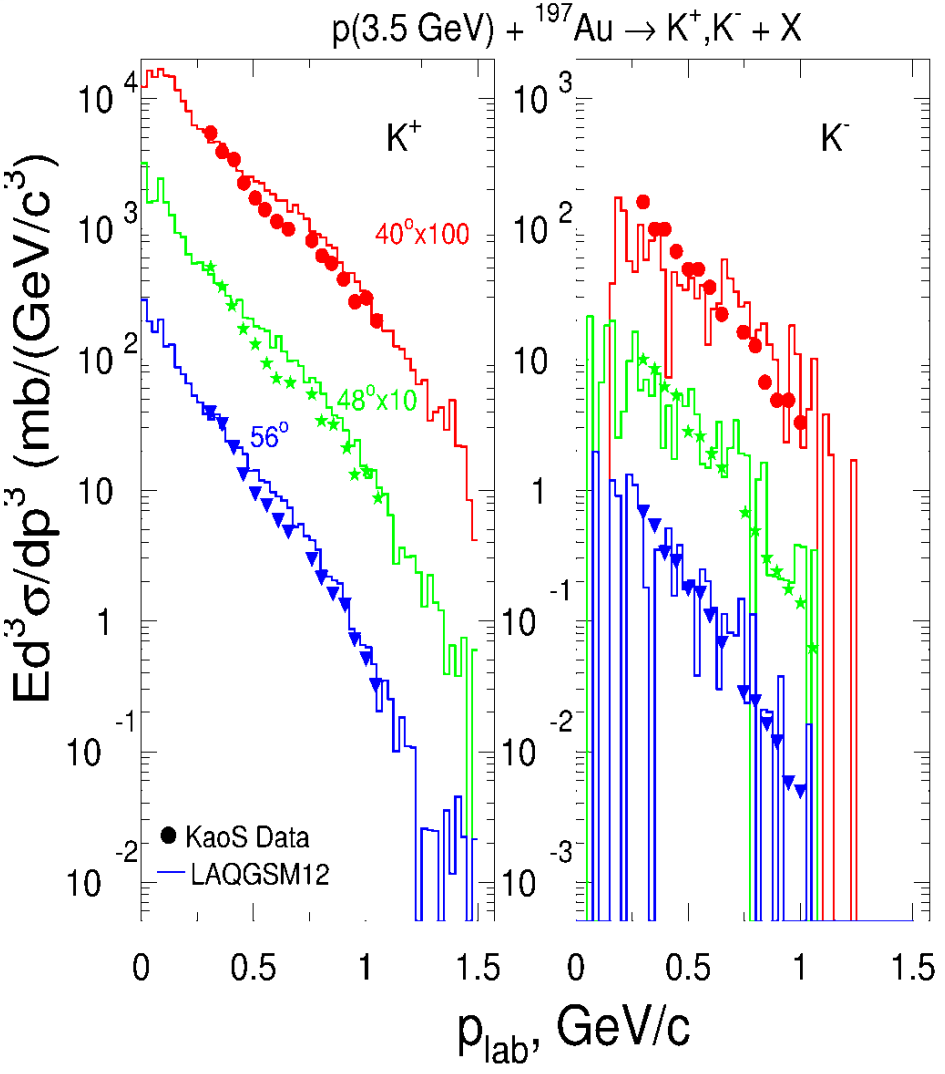

Fermilab

Mean Stopping Power

$$-\frac{1}{\rho}\frac{dE}{dx} = 4\pi N_A r_e^2 m_e c^2 z^2 \frac{Z}{A}\frac{1}{\beta^2} L(\beta)$$

$$L(\beta) = L_0(\beta) + \sum_i \Delta L_i$$

$$L_0(\beta) = \ln\left(\frac{2m_e c^2 \beta^2 \gamma^2}{I}\right) - \beta^2 - \frac{\delta}{2}$$

Bethe-Bloch formula

Continuous-slowing-down-approximation (CSDA)

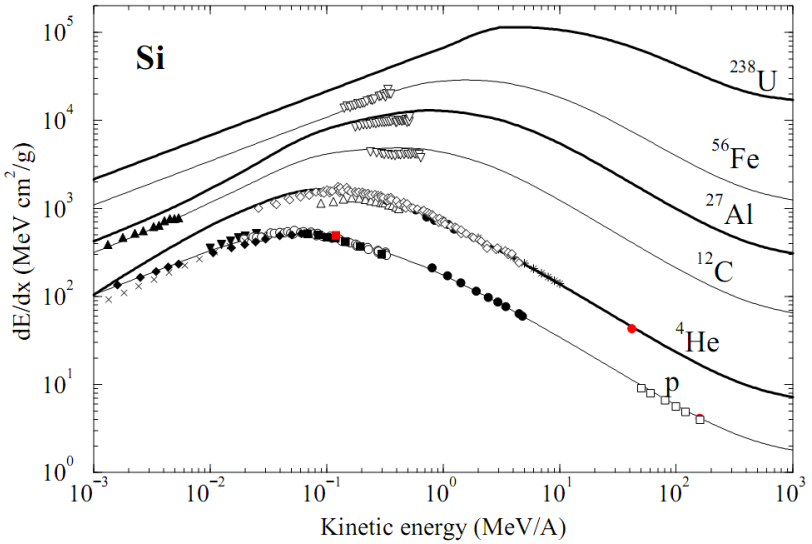

ΔLi: (i) **Lindhard-Sørensen** correction (exact solution to the Dirac equation; terms higher than z^2);

(ii) **Barkas** correction (target polarization effects due to low-energy distant collisions);

(iii) **shell** correction;

Projectile **effective charge** comes separately as a multiplicative factor that takes into account electron capture at low projectile energies (e.g., z_{eff} ~ 20 for 1-MeV/A ^{238}U in Al, instead of bare charge of 92).

Fermilab

dE/dx: Mixtures and Heavy Ions

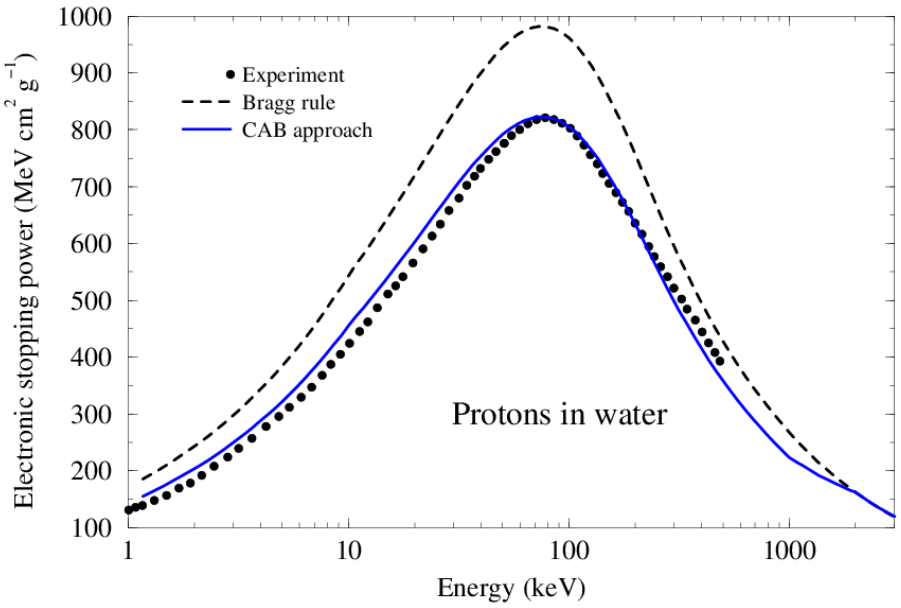

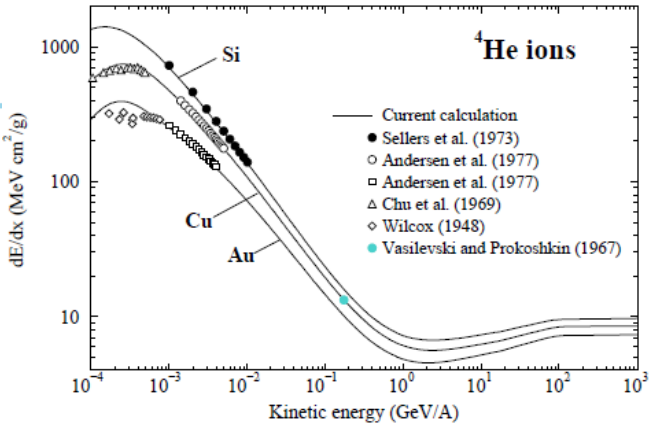

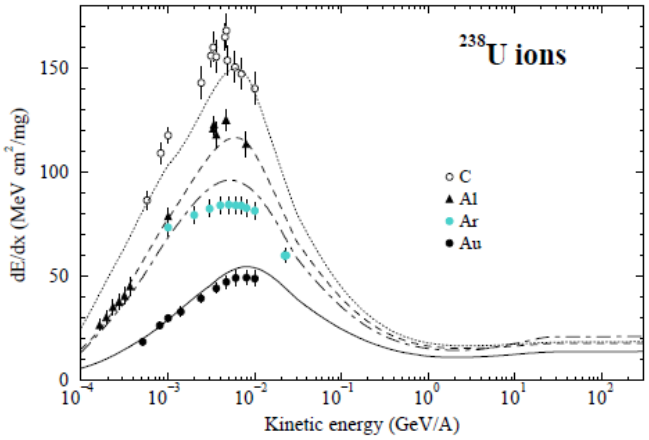

Stopping power of ions in compounds usually is described according to Bragg's rule. At low energies and for low-Z materials the difference between measured and predicted dE/dx can be as large as 20%. The "cores-and-bonds" (CAB) method in MARS15 takes into account chemical bonds fitted to experiment for various compounds

Energy Loss and Energy Deposition Modeling

1. The CSDA dE/dx is widely used in quick estimations of energy loss by particle beams and in simplified simulations of **energy loss and energy deposition** along the charged particle tracks in hadronic and electromagnetic cascades.
2. In a more sophisticated approach used in MARS15, precise modeling of knock-on electron production with energy-angle correlations taken into account is done for electronic losses.

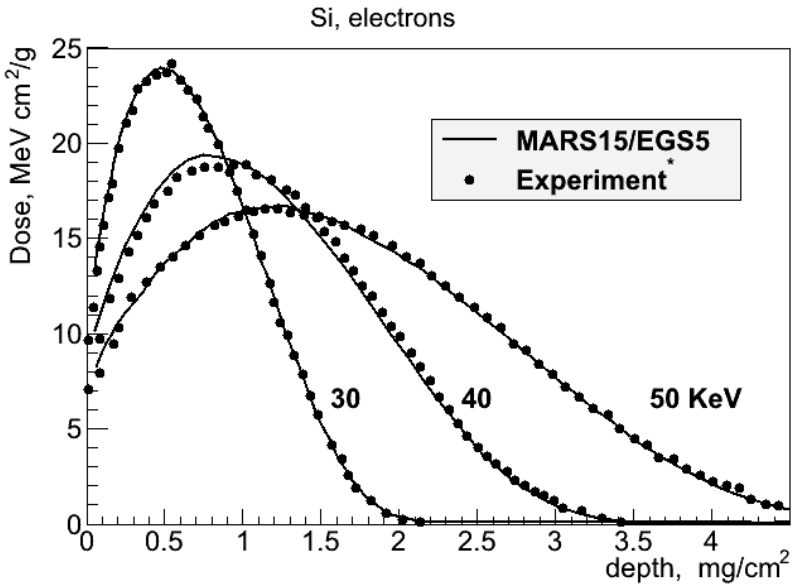

3. Radiative processes – bremsstrahlung, pair production and inelastic nuclear interactions (via virtual photon) – for muons and high-energy hadrons - are modelled exclusively using pointwise x-sections.

Items (2) and (3) allow precise calculation of 3D energy deposition maps induced by high energy cascades.

Atomic Displacements (DPA) in MARS15

- Atomic displacement cross-section σ_{DPA} is a reference way to characterize the radiation damage induced by neutrons and charged particles in crystalline materials. To evaluate a number of displaced atoms, Norget, Torrens and Robinson proposed in 1975 a standard NRT-DPA, which has been widely used since

$$DPA(t) = \iiint \Sigma_{DPA}(\vec{r}, E)\, \Phi\left(\vec{r}, \vec{\Omega}, E, t\right) d\vec{r}\, d\vec{\Omega}\, dE$$

- Energy of recoil fragments and new charge particles in (elastic and inelastic) nuclear interactions is used to calculate atomic displacement cross sections σ_{DPA} for the NRT model – w/o or with Nordlund/Stoller damage efficiency ξ(T) – for a number of stable defects
- Atomic screening parameters are calculated using the Hartree-Fock form-factors and recently suggested corrections to the Born approximation
- NJOY2016+ENDF/B-VIII.0(2018) was used to generate an NRT/Nordlund/Stoller database for 490 nuclides for neutrons from 10^{-5} eV to 200 MeV; DPA in neutron-nuclear interactions above 200 MeV are treated the same way as described in the second bullet

Atomic Displacement Cross-Section and NIEL

- Atomic displacement cross section

$$\sigma_d = \sum_r \int_{E_d}^{T_r^{\max}} \frac{d\sigma(E, Z_t, A_t, Z_r, A_r)}{dT_r} N_d(T_r, Z_t, A_t, Z_r, A_r) dT_r$$

- N_d – number of stable defects produced, E_d –displacement threshold, $d\sigma/dT_r$ - recoil fragment energy (T_r) distribution

- Non-ionizing energy loss (NIEL)

$$\frac{dE}{dx}_{ni} = N \sum_r \int_{E_d}^{T_r^{\max}} \frac{d\sigma(E, Z_t, A_t, Z_r, A_r)}{dT_r} T_d(T_r, Z_t, A_t, Z_r, A_r) dT_r$$

N – number of atoms per unit volume

T_d - damage energy=total energy lost in non-ionizing process (atomic motion)

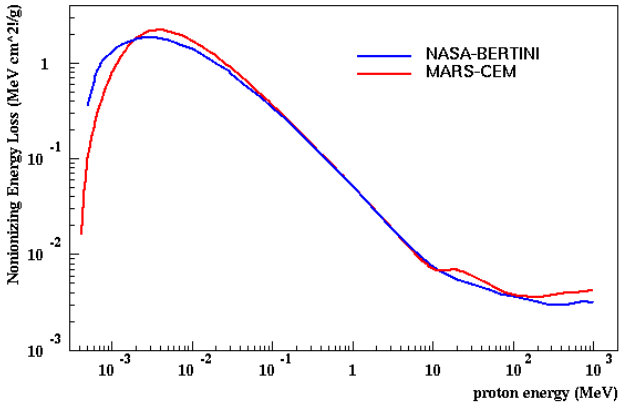

Recoil Energy Distributions

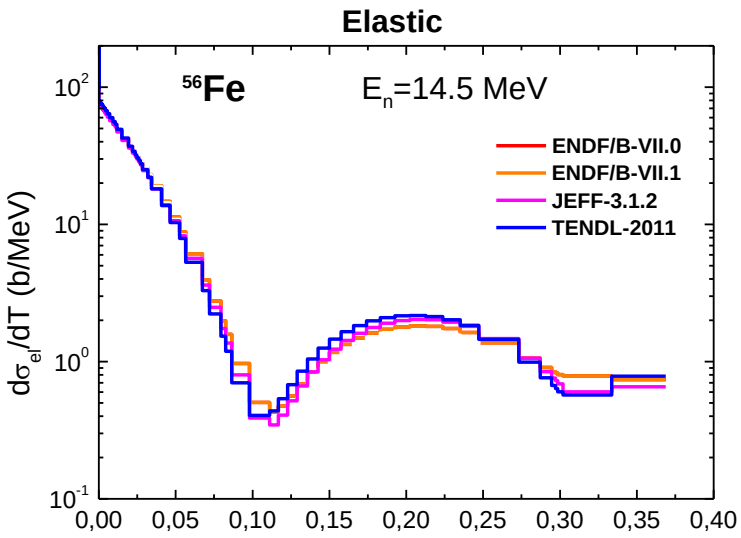

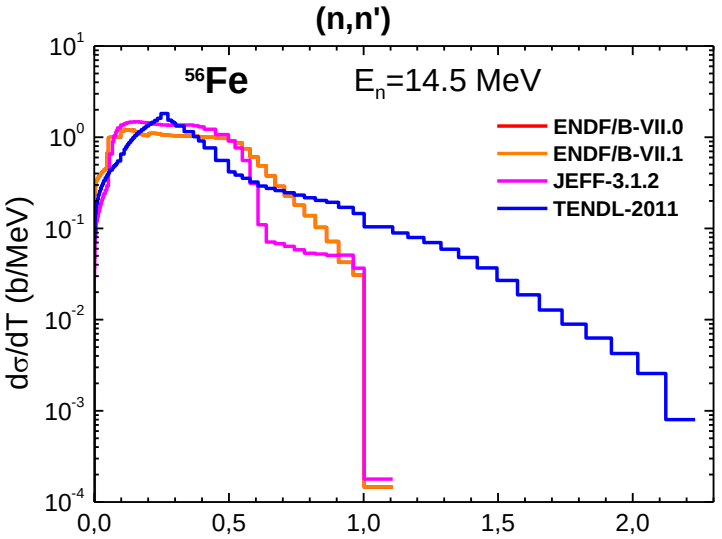

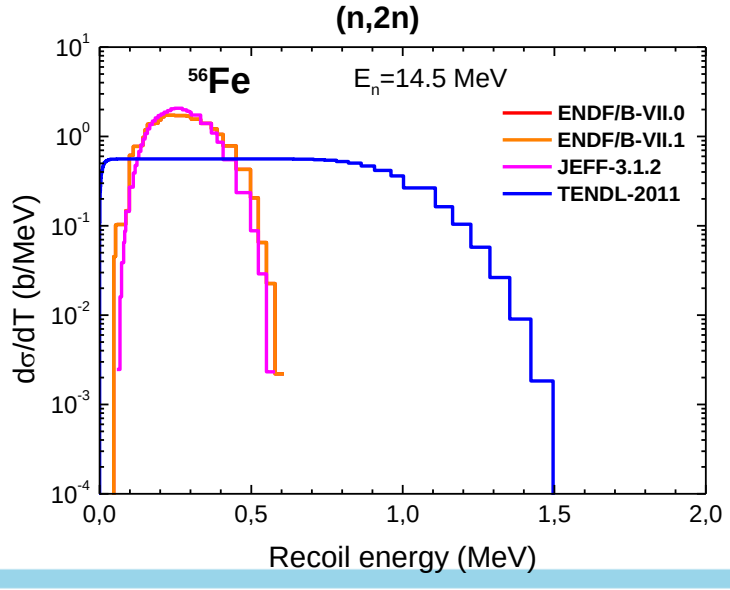

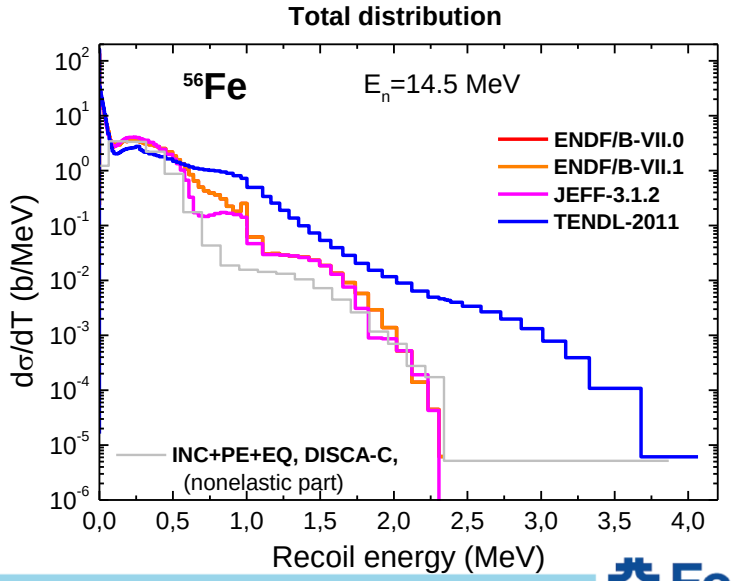

Fermilab

NRT "Standard" Model to Calculate a Number of Frenkel Pairs and Damage Energy

M.J. Norgett, M.T. Robinson, I.M. Torrens Nucl. Eng. Des 33, 50 (1975)

$$N_d = \frac{0.8}{2E_d} T_d$$

$$T_d = \frac{T_r}{1 + k(Z_t, A_t, Z_r, A_r) g(T_r, Z_t, A_t, Z_r, A_r)}$$

T_r, Z_r, A_r - recoil fragment energy=primary knock-on (PKA) energy, charge and atomic mass

Z_t, A_t - charge and atomic mass of irradiated material

Nuclear physics (T_r, T_d) + solid state physics (N_d)

NRT-DPA is successfully applied to correlate data from many studies involving direct comparison from different irradiation environments

Efficiency Function (1): Stoller MD Parametrization

Corrections to NRT to account for atom recombination in elastic cascading. Database based on MD simulations. Its parametrization, efficiency function $\xi(T)=N_D/N_{NRT}$, is used for several years in MARS15 (=1 if >1, since 2016).

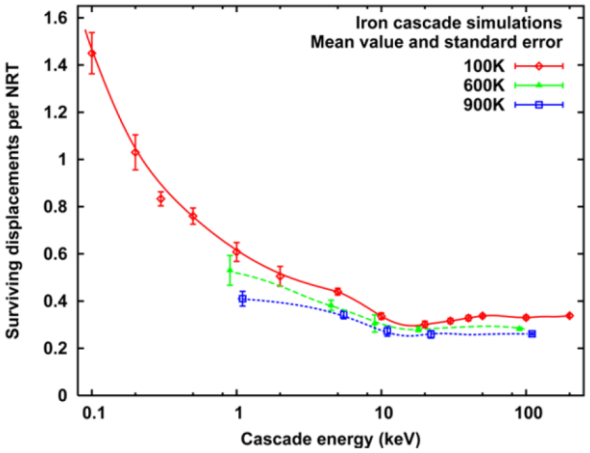

Temperature dependence. The calculations of Stoller (J. Nucl.Mater. 276 (2000) 22) for iron at 100-900K show some temperature dependence of the number of stable defects. At the same time the comparison of displacement cross-sections for p+Fe calculated using Stoller defect generation efficiency with the displacement cross-sections derived by Jung (J. Nucl. Mater. 117 (1983) 70) from low temperature experiments shows very good agreement.

Efficiency Function (2): Nordlund ARC-DPA

Nordlund's the ARC-DPA concept (athermal recombination-corrected DPA, in MARS15 since 2016):

"The recombination process does not require any thermally activated defect migration (atom motion is caused primarily by the high kinetic energy introduced by the recoil atom), this recombination is called "athermal" (i.e. it would also happen if the ambient temperature of the sample would be 0 K)."

The arc-dpa concept allows empirical validation against frozen defects at cryogenic temperature (whereas NRT is an unobservable quantity)."

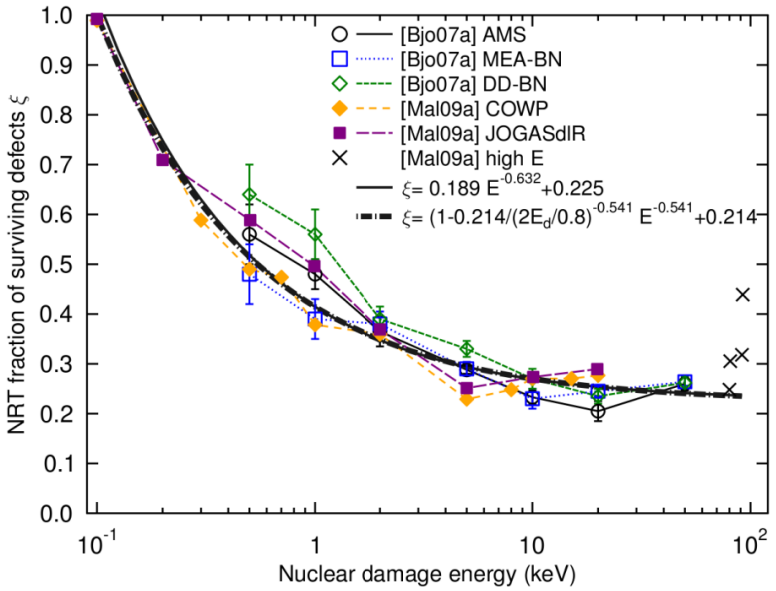

Modified NRT

$$N_d = \begin{cases} 0 & T_d < E_d \\ 1 & E_d < T_d < 2.5E_d \\ \dfrac{T_d}{2.5E_d}\xi(T_d) & 2.5E_d < T_d \end{cases}$$

with efficiency function

$$\xi(T) = 0.214 + 0.786 \times (2.5E_d / T)^{0.541}$$

Experimental Data Relevant to DPA Analysis

Jung et al, Greene et al and Iwamoto measured electrical resistivity change due to protons, electrons, light ions, fast and low-energy neutrons at low temperatures and low doses. It is connected to displacement cross section σ_d

$$\Delta\rho_d(\Phi, E) = \Phi\ \sigma_d(E)\rho_F$$

ρ_F is a resistivity per unit concentration of Frenkel defects. This constant cannot be accurately calculated and is determined phenomenologically. Jung and Greene groups choose different ρ_F (μΩm/u.c.) for the same material

	Jung	Greene	Iwamoto
Cu	2.5 ± 0.3	2	2 ± 1
W	27 ± 6	14	-

Konobeev, Broeders and Fisher (IOTA) note that Greene's choice for W seems questionable, taking into account later analysis

Proton and Neutron DPA Verification

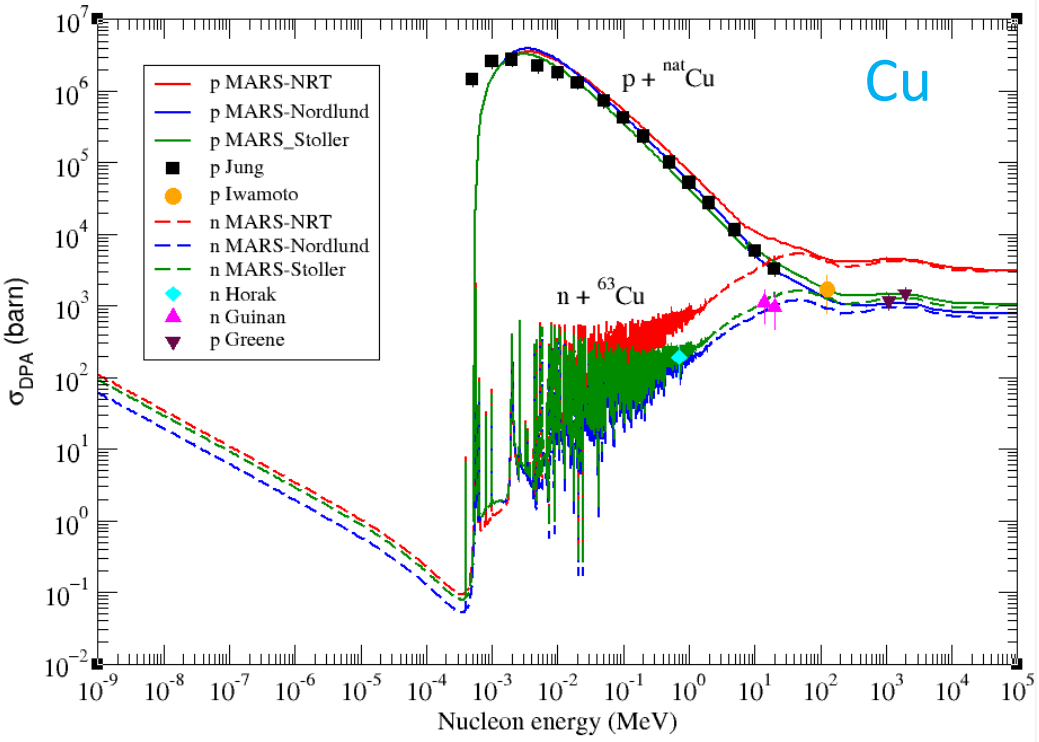

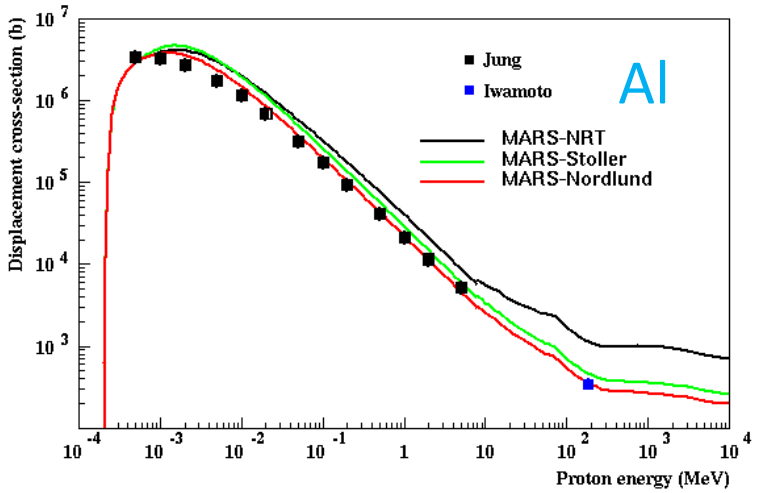

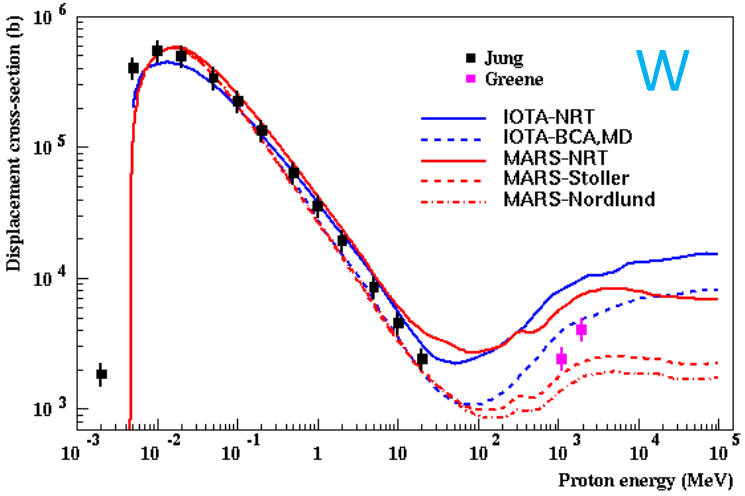

Ti-Window: EDEP @ 2, 180, 800 MeV and 3 GeV

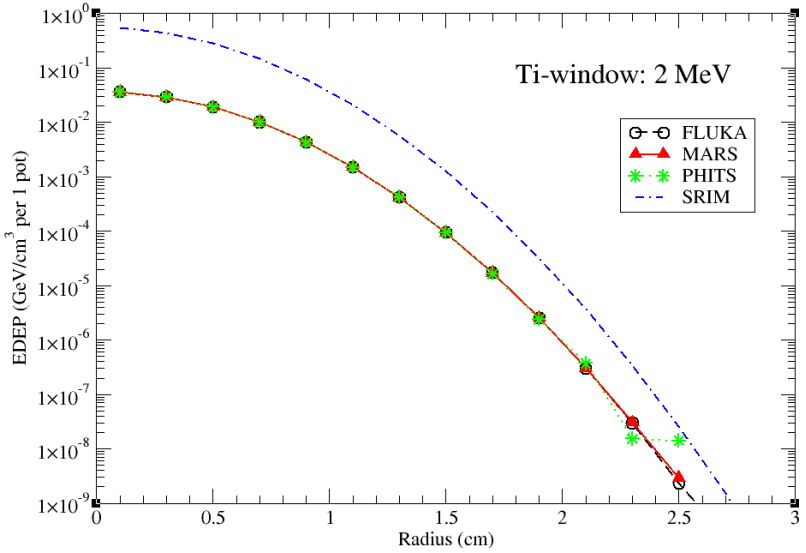

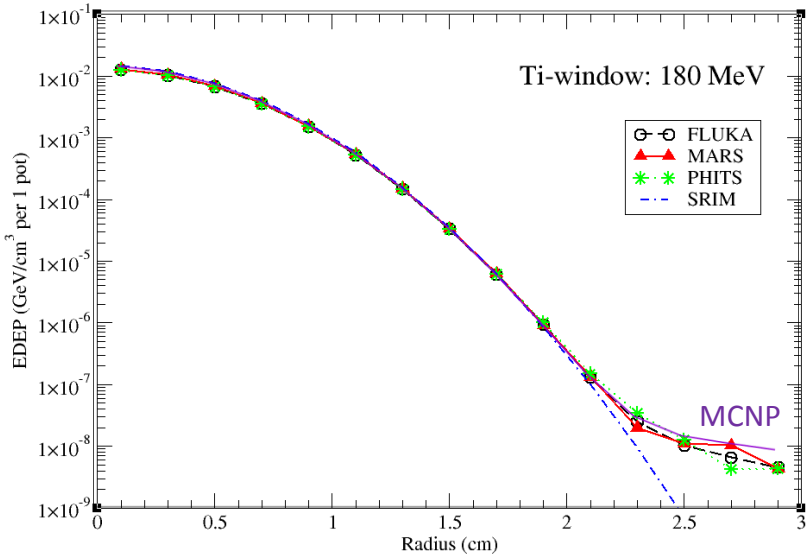

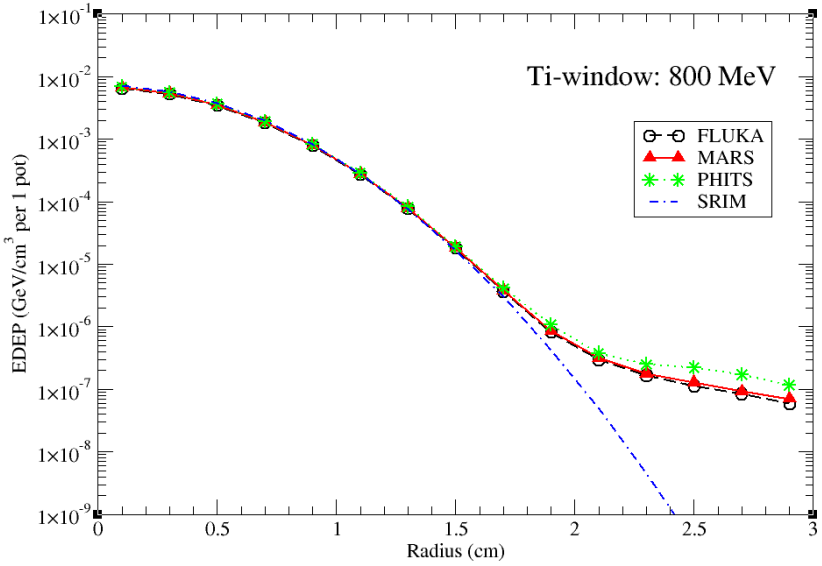

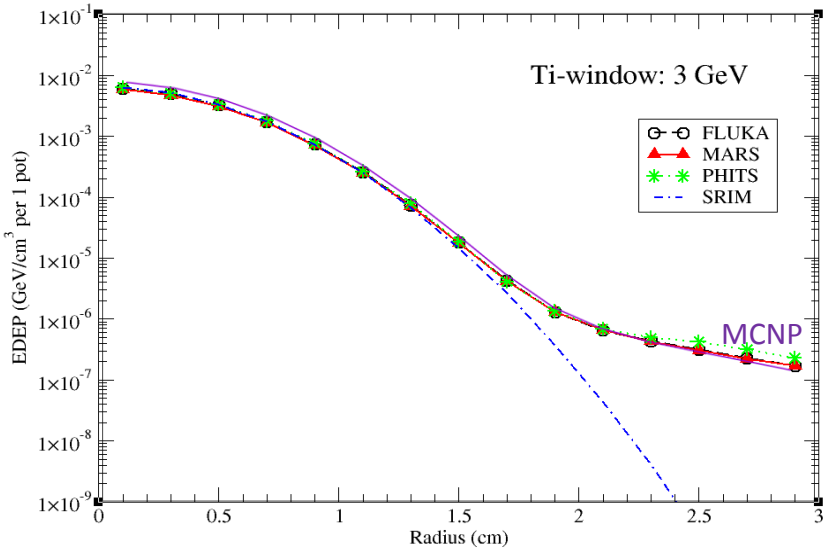

Ti-Window: EDEP @ 30, 120, 400 and 7000 GeV

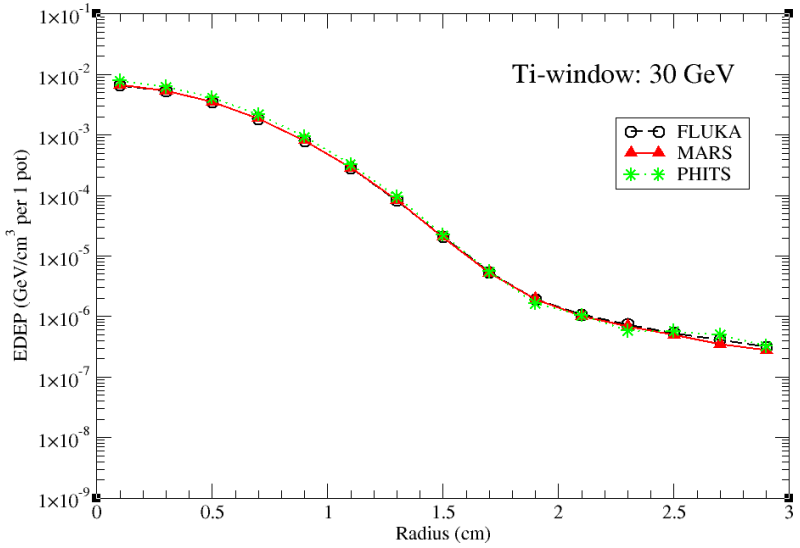

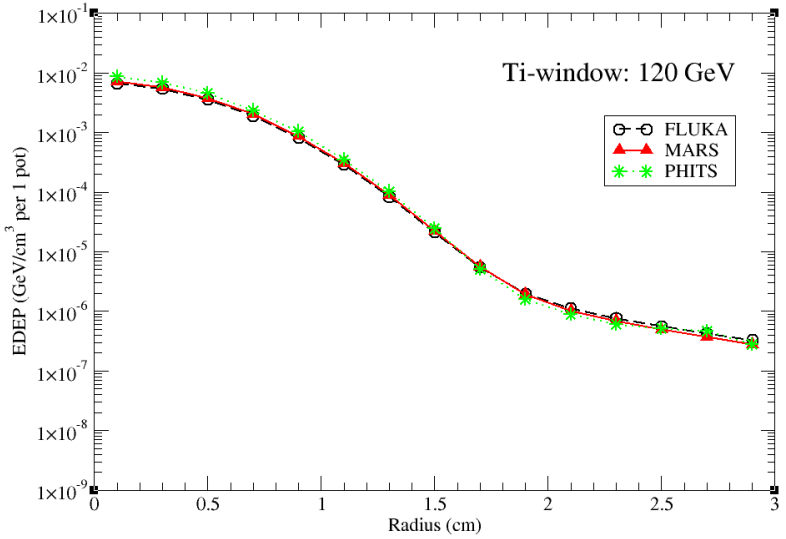

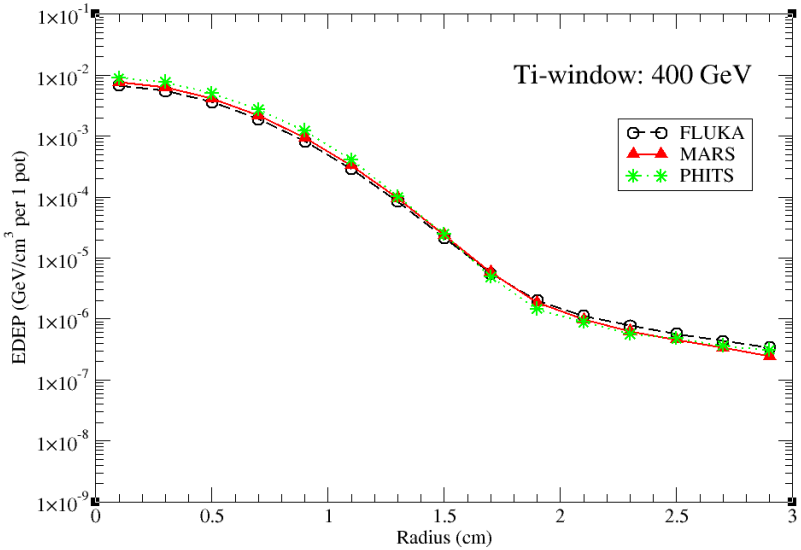

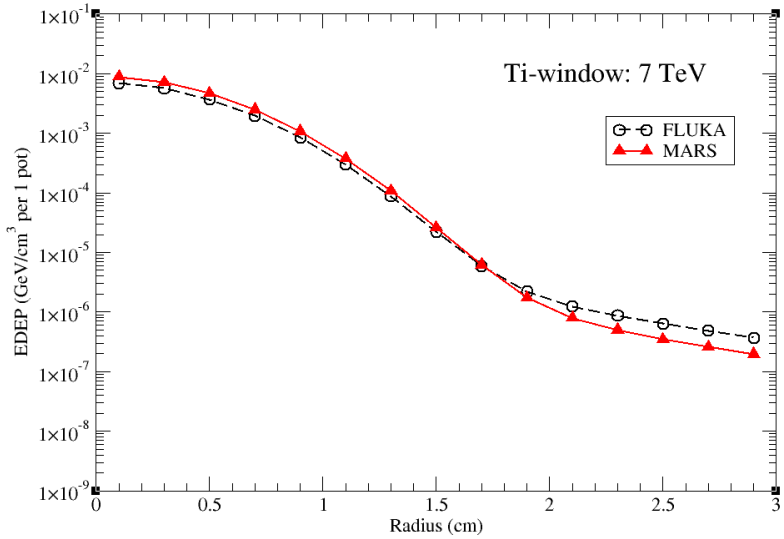

Ti-Window: DPA @ 2, 180, 800 MeV and 3 GeV

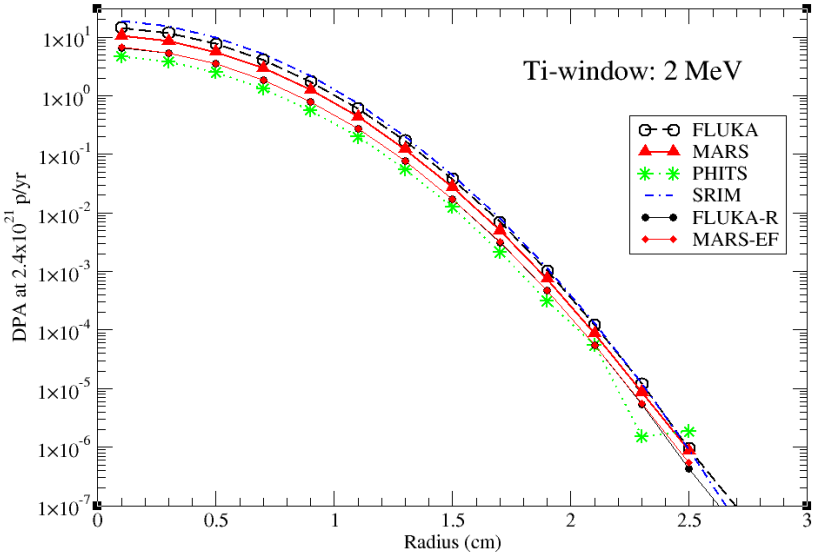

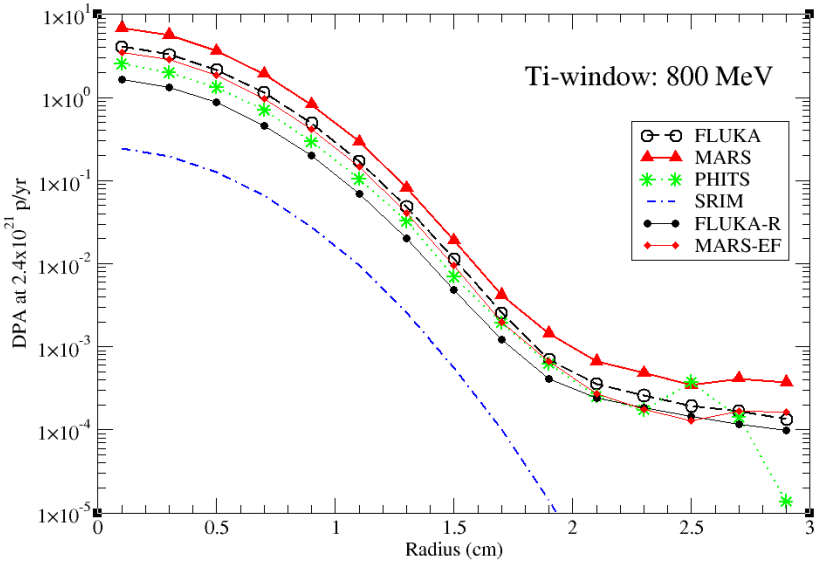

Use FLUKA-R and MARS-EF

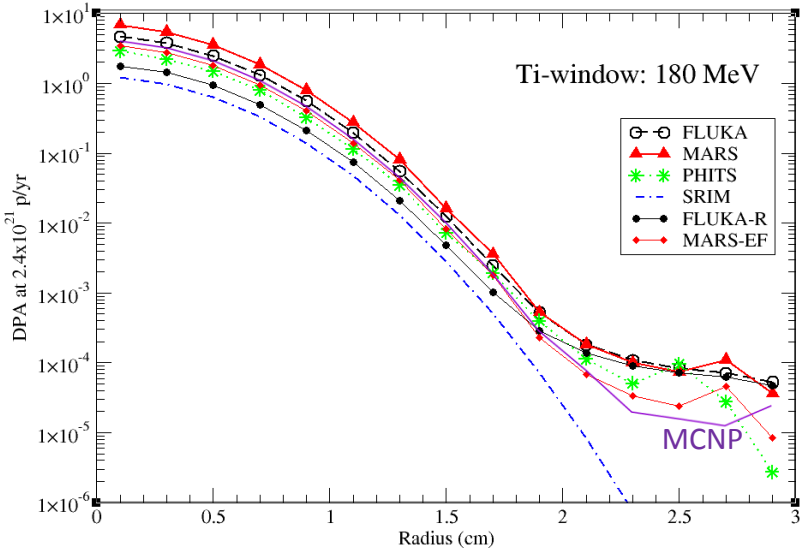

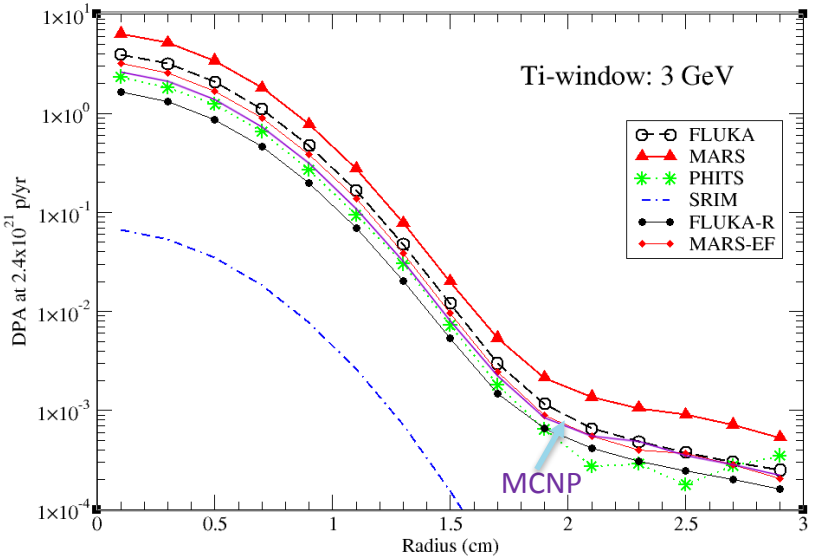

Ti-Window: DPA @ 30, 120, 400 and 7000 GeV

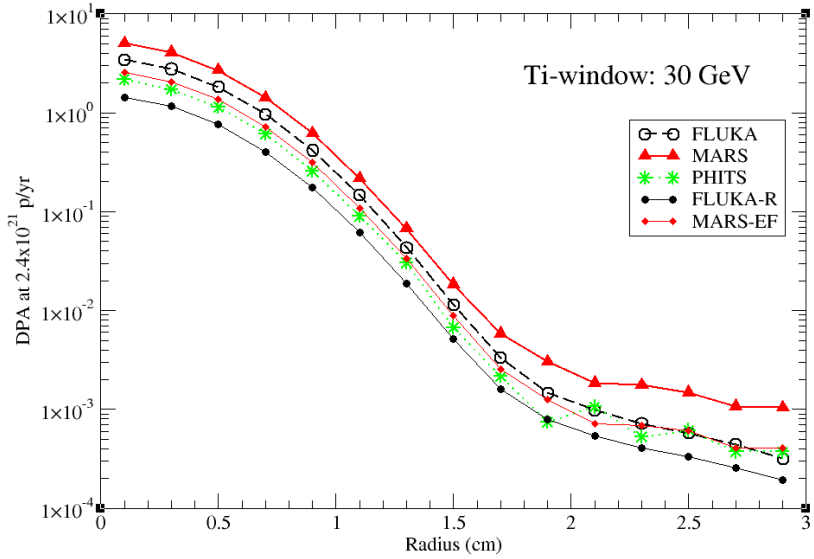

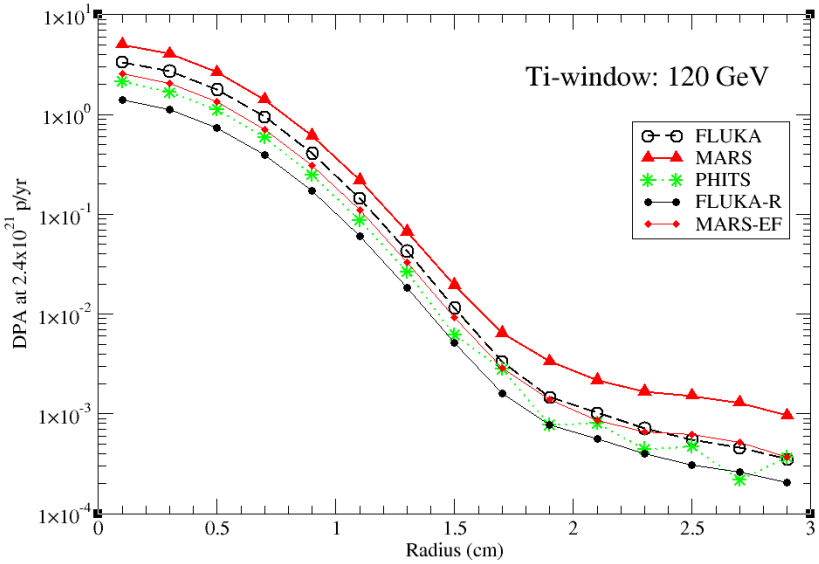

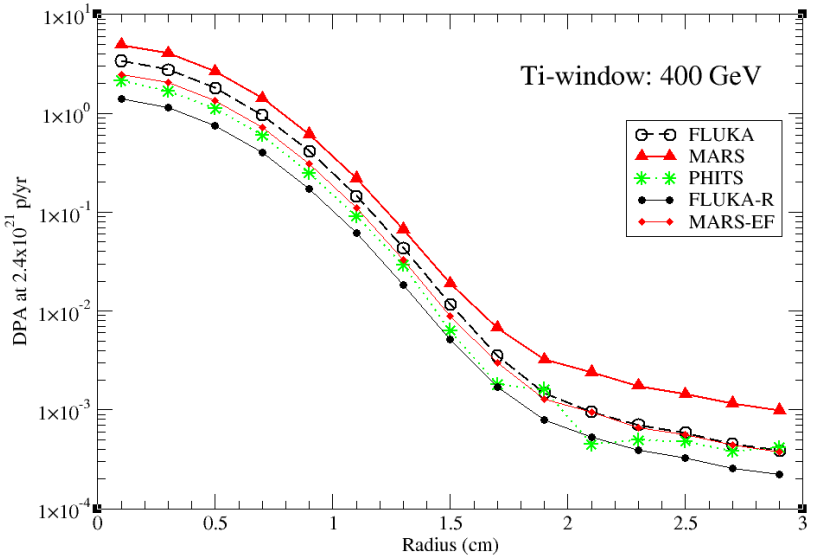

Use FLUKA-R and MARS-EF

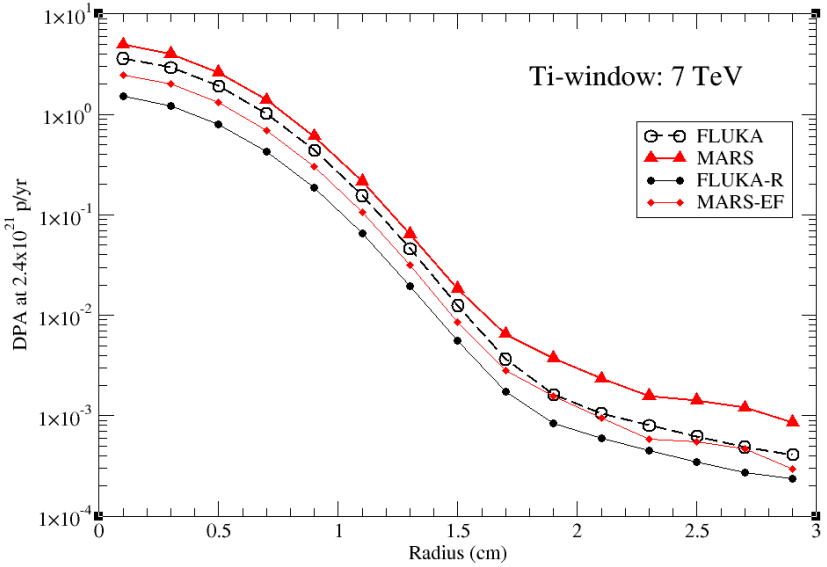

C-Target: EDEP @ 3 and 30GeV

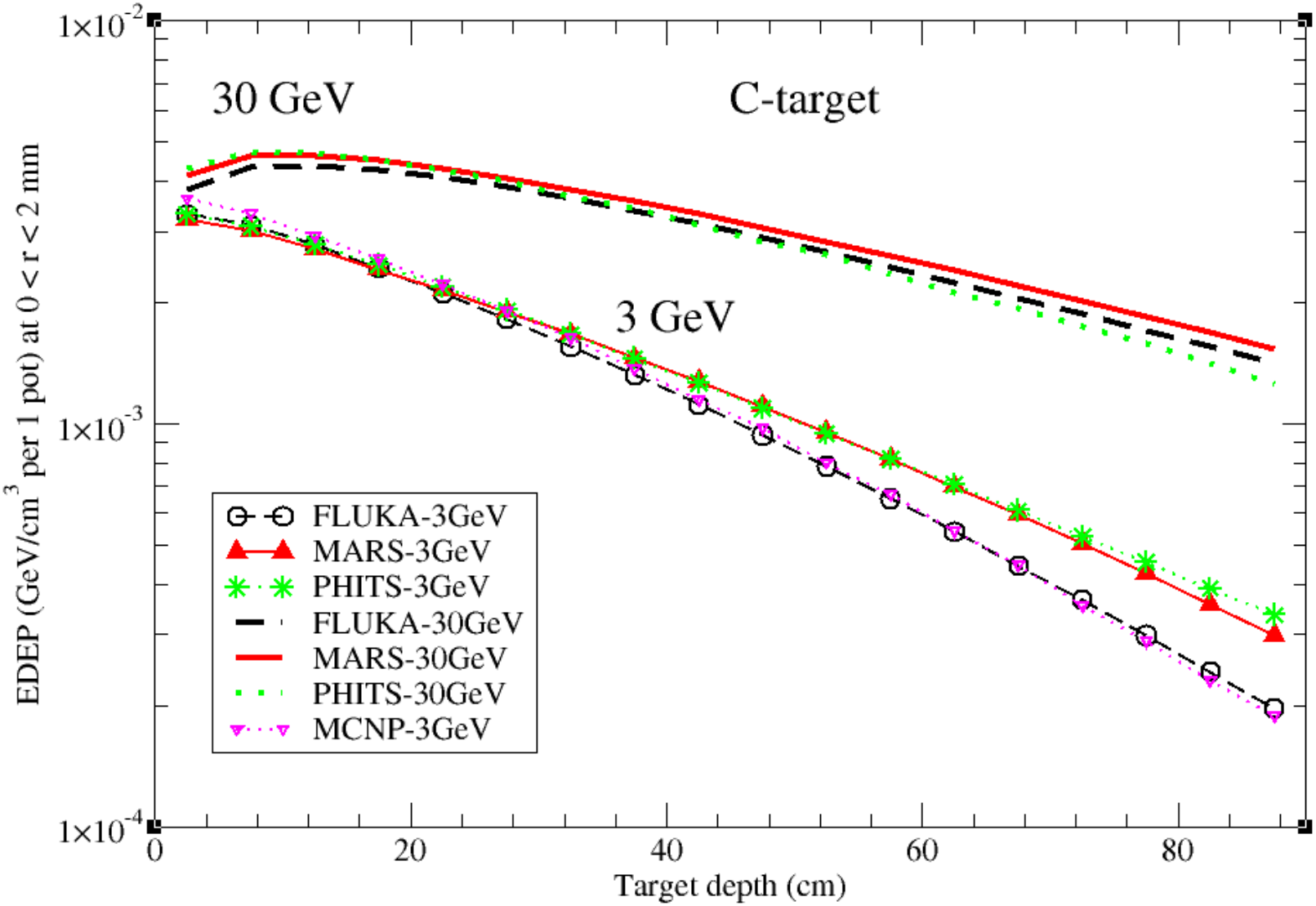

C-Target: EDEP @ 120, 400 and 7000 GeV

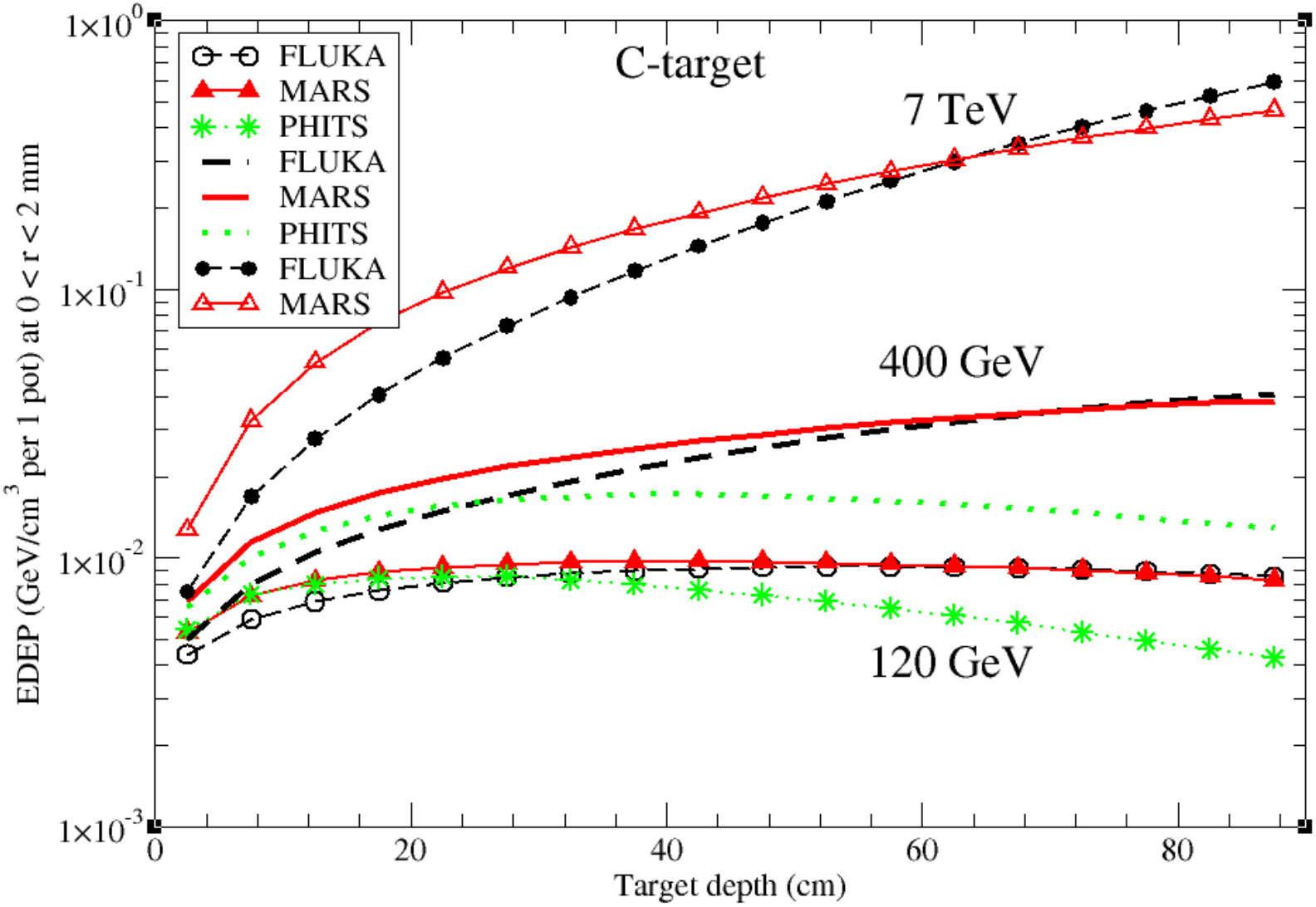

Fermilab

C-Target: DPA @ 180, 800 MeV, 3 GeV and 120 GeV

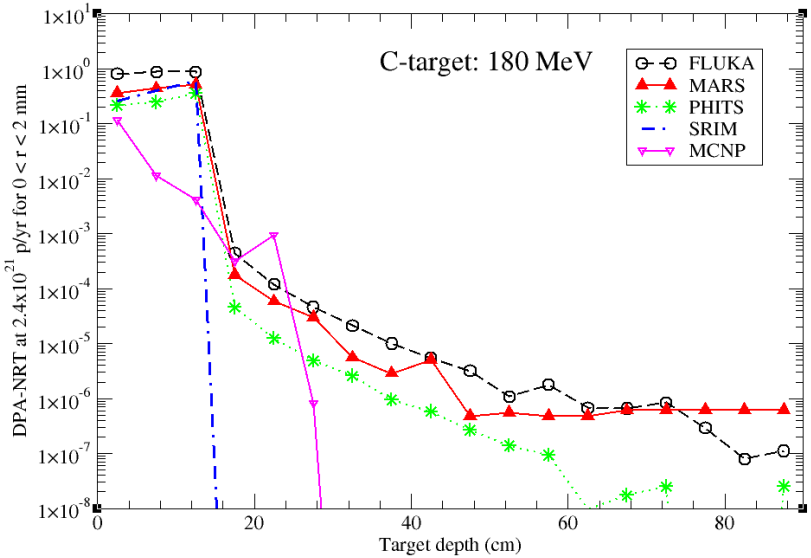

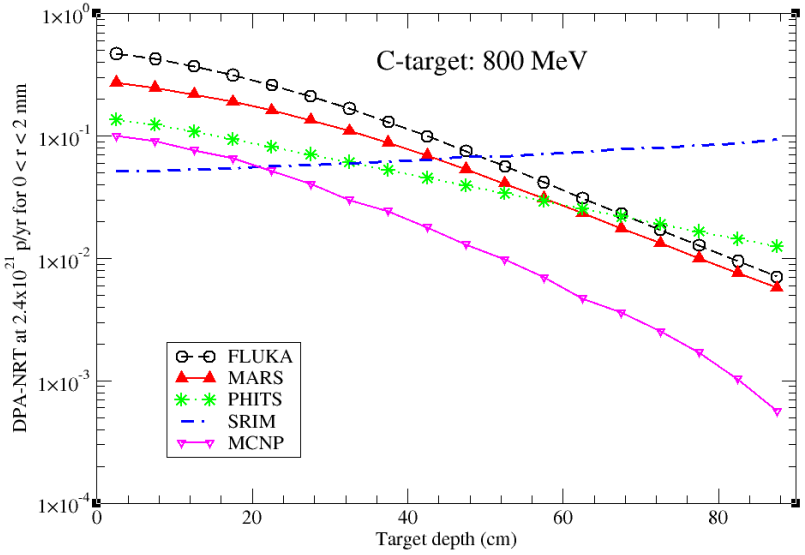

Use FLUKA-R and MARS-EF

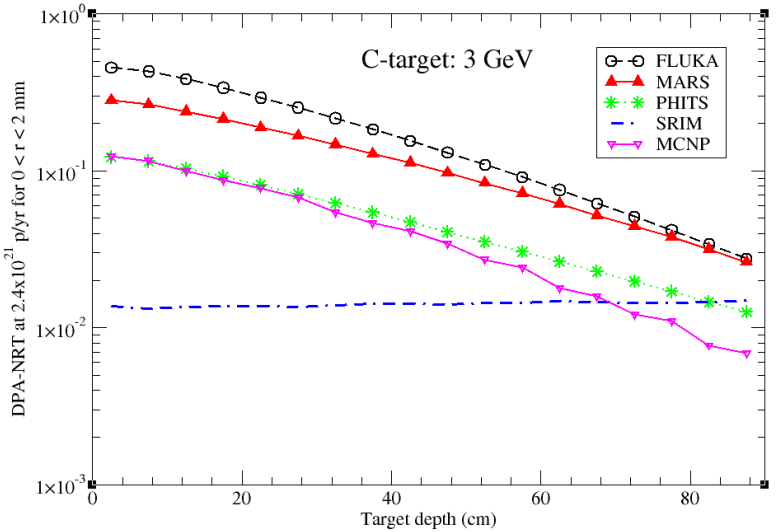

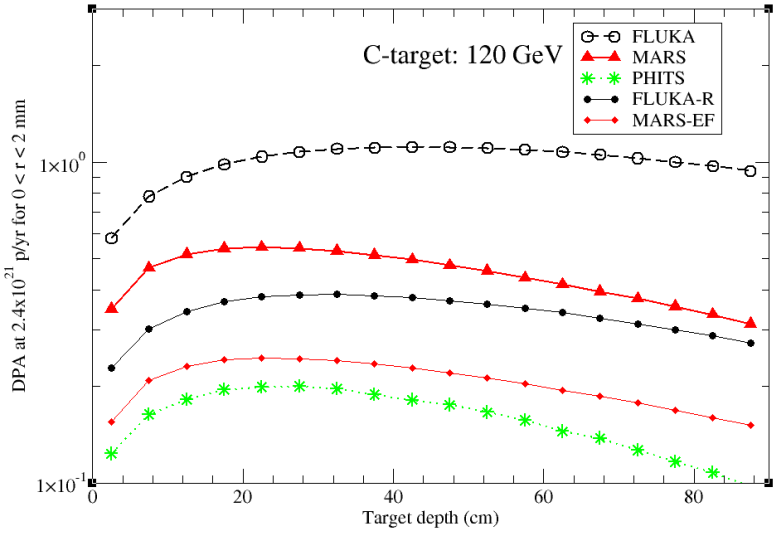

C-Target: He appm/DPA at r < 2 mm

Use FLUKA-R and MARS-EF

E_p	FLUKA	FLUKA-R	MARS	MARS-EF	PHITS	MCNP
180 MeV	1245.	1973.	788.	1614.	7.93	1290.
800 MeV	902.	1321.	1094.	2390.	11.90	466.
3 GeV	986.	2444.	1063.	2500.	13.82	203.
30 GeV	855.	2243.	1100.	2490.	25.59	-
120 GeV	881.	2279.	1074.	2390.	35.65	-
400 GeV	860.	2265.	1074.	2355.	28.23	-
7 TeV	899.	2309.	1116.	2507.	-	-

The He appm/DPA ratio longitudinal distributions at r < 2mm in the target are pretty flat, therefore just maxima of the ratio are shown in the table

Thermal Shocks

Short pulses with energy deposition density EDD in the range from 200 J/g (W), 600 J/g (Cu), ~1 kJ/g (Ni, Inconel) to ~15 kJ/g: thermal shocks resulting in fast ablation and slower structural changes.

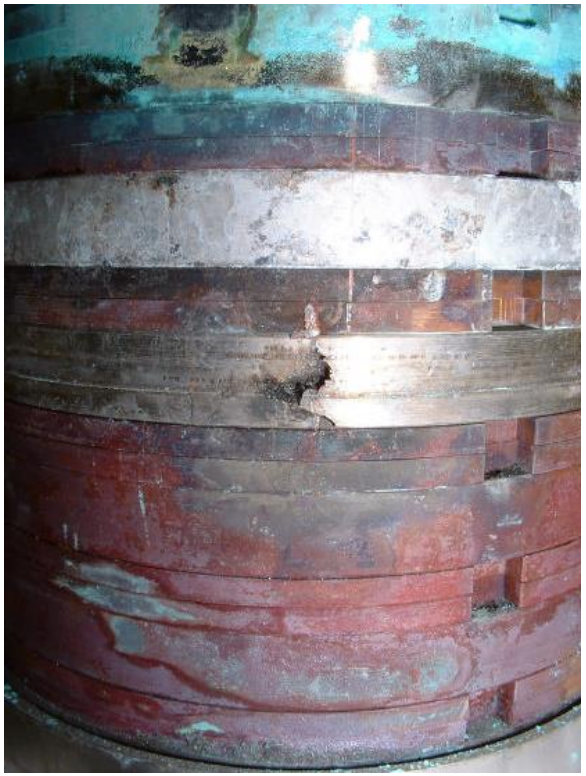

FNAL pbar production target under 120-GeV p-beam (3e12 ppp, σ ~ 0.2 mm)

MARS simulations explained reduction of pbar yield and justified better target materials

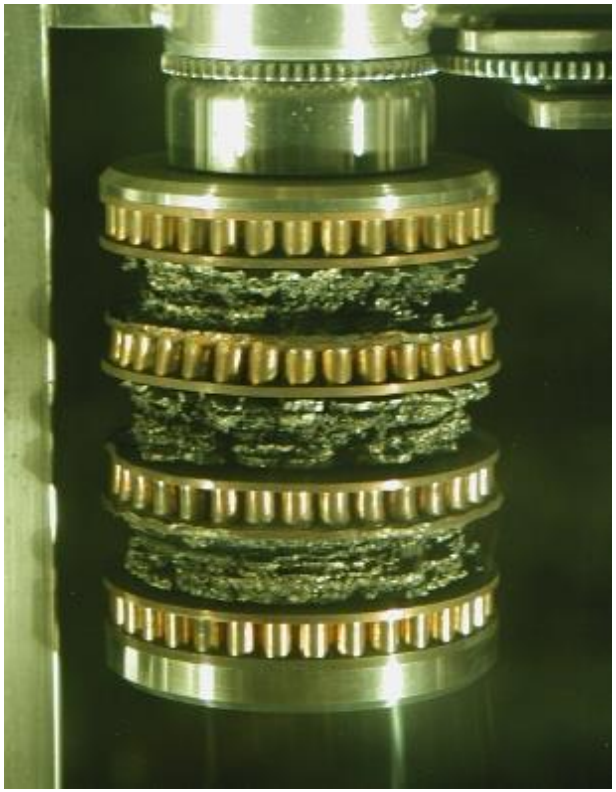

Tevatron Beam Accident (2003): Collimator Ablation

Hole in 5-mm W

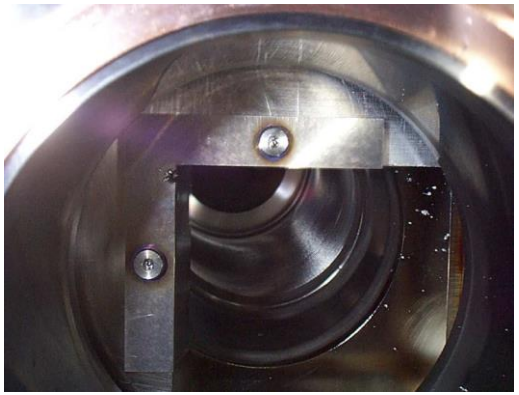

25-cm groove in SS

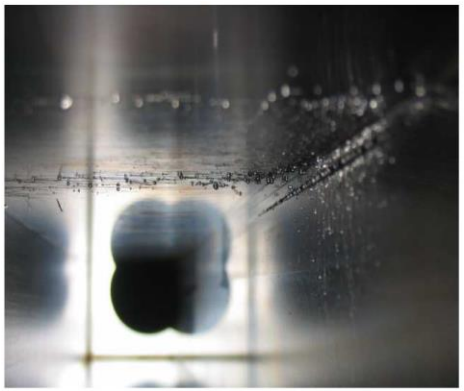

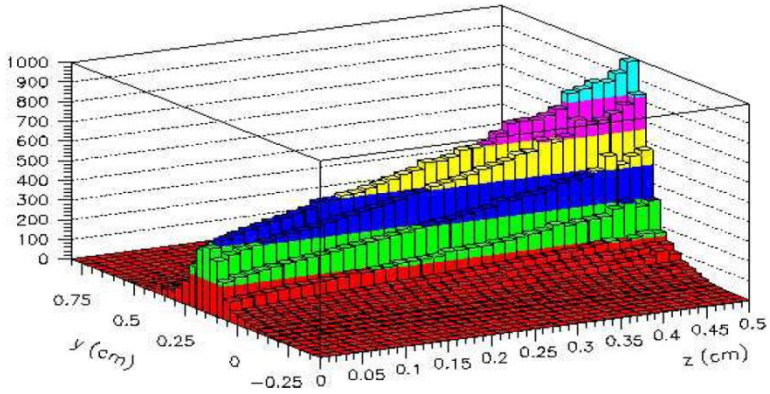

Detailed modeling of dynamics of beam loss (STRUCT), energy deposition (MARS15) as high as 1 kJ/g, and time evolution over 1.6 ms of the tungsten collimator ablation, fully explained what happened

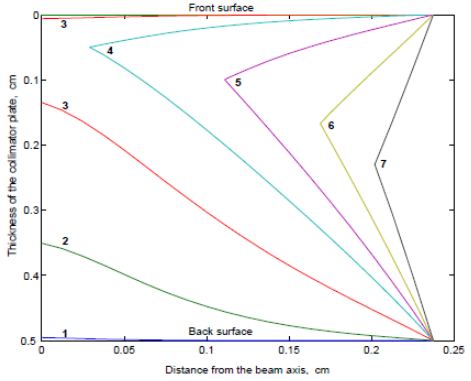

Figure 7: Evolution of the front and back surfaces of the collimator plate at $t = 0.4_{[1]} - 1.6_{[7]}\ ms$ with Δt=0.2 ms.

980-GeV p-beam

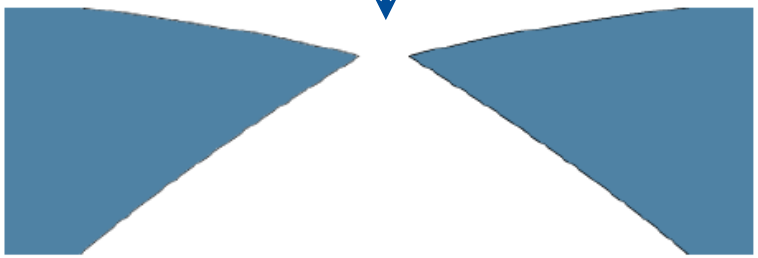

Fermilab

Hydrodynamic Tunneling in Solid Materials

Pulses with EDD >15 kJ/g: hydrodynamic regime

First calculated for the 300-μs, 400-MJ, 20-TeV proton beams for the SSC graphite beam dump, steel collimators and tunnel-surrounding Austin Chalk by SSC-LANL Collaboration (D. Wilson, …, N. Mokhov, PAC93, p. 3090). Combining MARS ED calculations at each time step for a fresh material state and MESA/SPHINX hydrodynamics codes.

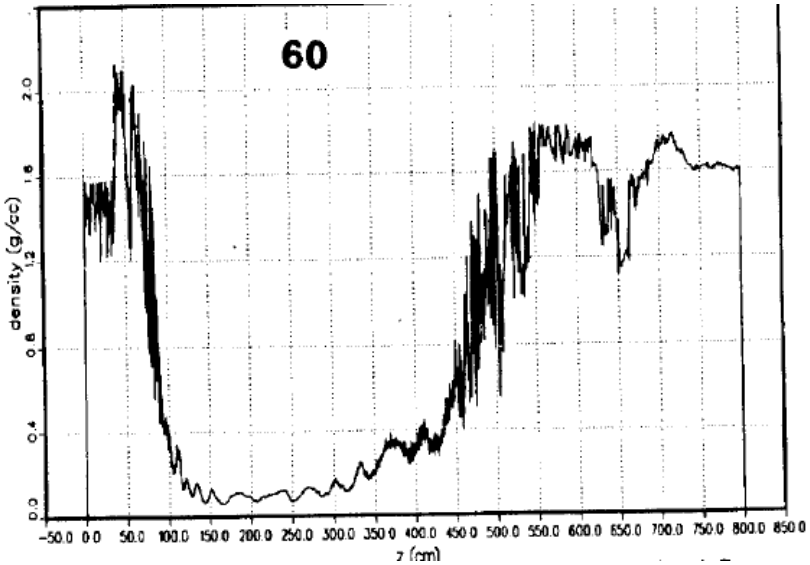

The hole was drilled at the 7 cm/μs penetration rate. Shown is axial density of graphite beam dump in 60 μs after the spill start

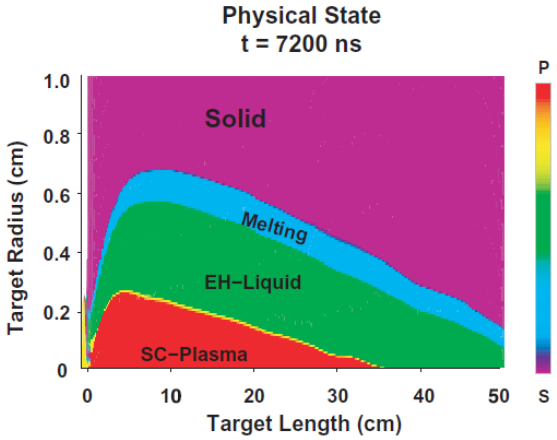

Later, studies by N. Tahir et al with FLUKA+BIG2 codes for SPS & LHC

These days we use MARS+FRONTIER